

8 **Very Long Period Oscillations in the Atmosphere**
9 **(0 – 110 km)**

10
11 Dirk Offermann(1), Christoph Kalicinsky(1), Ralf Koppmann(1), and Johannes
12 Wintel(1,2)
13
14
15
16

- 17 (1) Institut für Atmosphären - und Umweltforschung, Bergische Universität Wuppertal,
18 Wuppertal, Germany
19 (2) Now at Elementar Analysensysteme GmbH, Langenselbold, Germany
20
21
22
23
24

25 Corresponding author: Dirk Offermann, (offerf@uni-wuppertal.de)
26
27
28

- 29 Key Points: - multi-decadal oscillations in GCM and measurements
30 - **oscillations related to the atmosphere basic dynamics**
31 - vertical amplitude and phase structure similar for all oscillation periods
32
33
34
35
36
37
38
39
40
41
42
43
44
45
46
47
48
49

50
51
52
53
54
55
56
57
58
59
60
61
62
63
64
65
66
67
68
69
70
71
72
73
74
75
76
77
78
79
80
81
82
83
84
85
86
87
88
89
90
91
92
93
94
95
96
97
98
99
100

Abstract

Multi-annual oscillations have been observed in measured atmospheric data. These oscillations are also present in General Circulation Models even if their boundary conditions with respect to solar cycle, sea surface temperature, and trace gas variability are kept constant. **They are therefore suspected to be self-generated.** The present analysis contains temperature oscillations with periods from below 5 yr up to above 200 yr in an altitude range from the Earth's surface to the lower thermosphere (110 km). The periods are quite robust as they are found to be the same in different model calculations and in atmospheric measurements. The oscillations show vertical profiles with special structures of amplitudes and phases. They form layers of high / low amplitudes that are a few dozen km wide. Within the layers the data are correlated. Adjacent layers are anticorrelated. A vertical displacement mechanism is indicated with displacement heights of a few 100 metres. Vertical profiles of amplitudes and phases of the various oscillation periods as well as their displacement heights are surprisingly similar. The oscillations are related to the thermal and dynamical structure of the middle atmosphere. These results are from latitudes/longitudes in Central Europe.

Short summary

Atmospheric oscillations with periods up to several 100 years exist at altitudes up to 110 km. They are also seen in computer models (GCM) of the atmosphere. They are often attributed to external influences from the sun, from the oceans, or from atmospheric constituents. This is difficult to verify as the atmosphere cannot be manipulated in an experiment. However, a GCM can be changed **selectively!** Doing so we find that long period oscillations may be excited internally in the atmosphere.

1 Introduction

Multi-annual oscillations with periods between 2 and 11 years have frequently been discussed for the atmosphere and the ocean. Major examples are the Quasi-Biennial Oscillation (QBO), solar cycle related variations near 11 years and 5.5 years, and the El Nino/Southern Oscillation (ENSO). (For references see for instance Offermann et al., 2015.)

Self-excited oscillations in the ocean of such periods have been described for instance by White and Liu (2008). Possibly self-excited oscillations in the atmosphere with periods between 2.2 and 5.5 yr have been shown in a large altitude regime by Offermann et al. (2015). Their periods are surprisingly robust, i.e. there is little change with altitude. They are also present in general circulation models, the boundaries of which are kept constant.

Oscillations of much longer periods in the atmosphere and the ocean have also been reported. Biondi et al. (2001) found bi-decadal oscillations in local tree ring records that date back several centuries. Kalicinsky et al. (2016, 2018) recently presented a temperature oscillation near the mesopause with a period near 25 years which may be interpreted as a self-excited oscillation. Low-frequency oscillations (LFO) on local and global scales in the multi-decadal range (50-80 yr) have been discussed several times (e.g., Schlesinger and Ramankutty (1994); Minobe (1997); Polyakov et al.(2003); Dai et al.(2015); Dijkstra et al.(2005)). Some of these results were intensively discussed as internal variability of the atmosphere-ocean system, for instance as the internal interdecadal modes AMV (Atlantic Multidecadal Variability) and PDO/IPO (Pacific Decadal Oscillation/Interdecadal Pacific Oscillation) (e.g. Meehl et al., 2013; 2016; Lu et al., 2014; Deser et al., 2014; Dai et al., 2015.) Multidecadal variations (40-80 years) of Arctic-wide surface air temperatures were, however, related to solar variability by Soon (2005). Some of these long period variations have been traced backwards for two or more centuries (Minobe, 1997; Biondi et al., 2001; Mantua and Hare, 2002; Gray et al., 2004). Multidecadal oscillations have also been discussed extensively as internal climatic variability in the context of the long term climate change (temperature increase) in the IPCC AR5 Report (e.g. Flato et al., 2013).

Even longer periods of oscillations in the ocean and the atmosphere have also been reported. Karnauskas et al. (2012) find centennial variations in three general circulation models of the ocean. These variations occur in the absence of external forcing, i.e. they show internal variabilities on the centennial time scale. Internal variability in the ocean on a centennial scale is also discussed by Latif et al. (2013) on the basis of model simulations. Measured data of a 500 year quasi-periodic temperature variation are shown by Xu et al. (2014). They analyze a more than 5000 year long pollen record in East Asia. Very long periods are found by Paul and Schulz (2002) in a climate model. They obtain internal oscillations with periods of 1600-2000 years.

All long period oscillations cited here refer to temperatures of the ocean or the land/ocean system. It is emphasized that on the contrary the multi-annual oscillations described by Offermann et al. (2015) and those discussed in the present paper are properties of the atmosphere, and exist in a large altitude regime between the ground and 110 km altitude. They are not related to the ocean (see below).

In the present paper the work of Offermann et al. (2015) is extended to multi-decadal and centennial periods. Oscillations in the atmosphere are studied in three general circulation models. The analysis is locally constrained (Central Europe), but vertically extended up to 110 km. The model boundary conditions (sun, ocean, trace gases) are kept constant. The results of model runs with HAMMONIA, WACCM, and ECHAM6 were made available to us. They simulate 34 years, 150 years, and 400 years of atmospheric behavior, respectively. The corresponding results are compared to each other. Most of the analyses are performed for atmospheric temperatures.

151 For comparison, long duration measured data series are also analyzed. There is a data set
152 taken at the Hohenpeißenberg Observatory (47.8°N, 11.0°E) since 1783. Long term data have
153 been globally averaged by Hansen et al., (2010), and published as GLOTI data (Global Land
154 Ocean Temperature Index).

155 In Section 2 of this paper the three models are described and the analysis method is
156 presented. In Section 3 the oscillations obtained from the three models are compared. The
157 vertical structures of the periods, amplitudes, and phases of the oscillations are described. In
158 Section 4 the results are discussed. Section 5 gives a summary and some conclusions.

159
160
161

162 2 Model data and their analysis

163
164

165 2.1 Long-period oscillations and their vertical structures

166

167 In an earlier paper (Offermann et al., 2015) multi-annual oscillations with periods of about
168 2 - 5 years have been described at altitudes up to 110 km. These were found in temperature
169 data of HAMMONIA model runs (see below). They were present in the model even if the
170 model boundary conditions (solar irradiance, sea-surface temperatures and sea ice, boundary
171 values of green-house gases) were kept constant. Therefore they were tentatively interpreted
172 as “self-excited” oscillations. The periods were found to be quite robust as they did not
173 change much with altitude. The oscillations showed particular vertical structures of amplitudes
174 and phases. Amplitudes did not increase exponentially with altitude as they do with
175 atmospheric waves. They rather varied with altitude between maximum and near zero values
176 in a nearly regular manner. Phases showed jumps of about 180° at the altitudes of the
177 amplitude minima, and were about constant in between. There were indications of
178 synchronization of amplitudes and phases.

179 The periods analyzed in the earlier paper have been restricted to below 5.5 yr. Much longer
180 periods have been described in the literature. It is therefore of interest to see whether such
181 longer periods could also be “self-excited” in the models, and what their origin might be.

182 Figure 1 shows an example of such temperature structures for an oscillation with a period
183 of 17.3 ± 0.8 years obtained from the HAMMONIA model discussed below. This picture is
184 typical of the oscillations in Offermann et al. (2015) and of the oscillations discussed in the
185 present paper. The periods at the various altitudes are close to their mean value even though
186 the error bars are fairly large. There is no indication of systematic altitude variations, and
187 therefore the mean is taken as a first approximation. At some altitudes the periods could not
188 be determined (see Section 3.3). In these cases the periods were prescribed by the mean of the
189 derived periods (dash-dotted red vertical line, 17.3 yr) to obtain approximate amplitudes and
190 phases at these altitudes (see Offermann et al., 2015). Details of the derivation of periods,
191 amplitudes, and phases are given in Section 3.2.

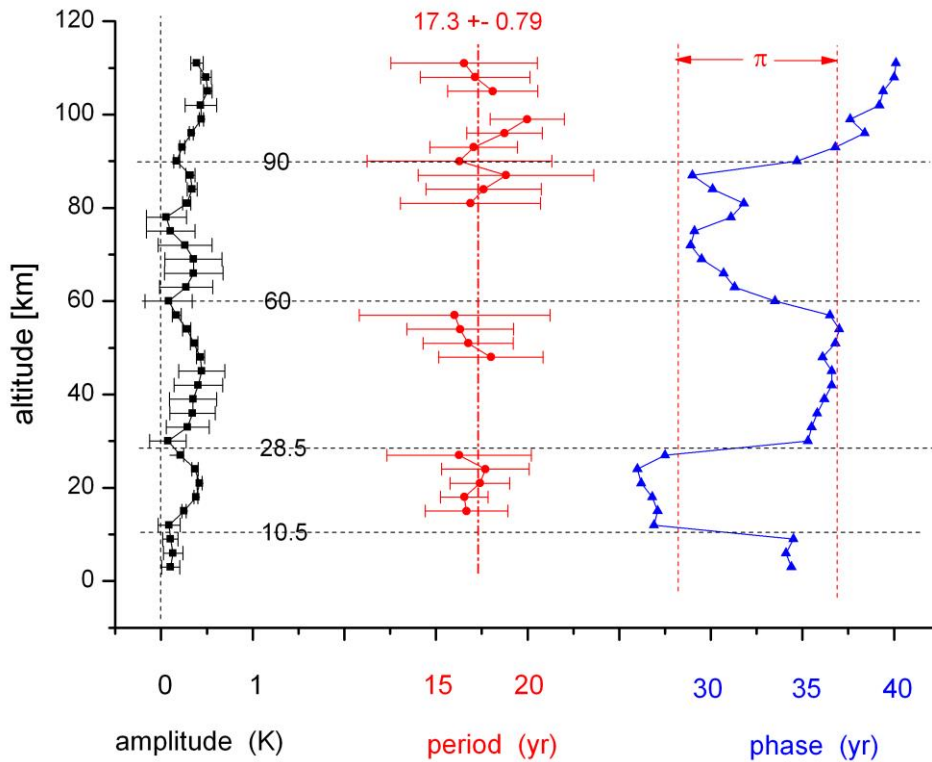
192
193

194 2.2 HAMMONIA

195

196 The HAMMONIA model (Schmidt et al., 2006) is based on the ECHAM5 general circulation
197 model (Röckner et al., 2006), but extends the domain vertically to 2×10^{-7} hPa, and is coupled
198 to the MOZART3 chemistry scheme (Kinnison et al., 2007). The simulation analyzed here
199 was run at a spectral resolution of T31 with 119 vertical layers. The relatively high

200
201



203

204

205 Fig. 1 Vertical structures of long-period oscillations near 17.3 ± 0.8 yr from HAMMONIA

206 temperatures.
 207 Missing period values could not be derived from the data. They were prescribed as the mean
 208 value 17.3 yr (dash-dotted vertical red line, see text and Section 3.2). Phases are relative
 209 values.

210

211 vertical resolution of less than 1 km in the stratosphere allows an internal generation of the
 212 QBO. Here we analyze the simulation (with fixed boundary conditions, including aerosol,
 213 ozone climatology) that was called “Hhi-max” in Offermann et al. (2015), but instead of only
 214 11 we use 34 simulated years. Further details of the simulation are given by Schmidt et al.
 215 (2010).

216

217 As concerns the land parameters, part of them were also kept constant (vegetation
 218 parameters as leaf area, wood coverage) and ground albedo. Others were not
 219 (e.g. snow and ice on lakes). Hence, some influence on our oscillations cannot be
 220 excluded. We, therefore, put the expression “self-excited” in quotation marks in this
 221 paper.

221

222 An example of the HAMMONIA data is given in Fig. 2 for 0 km and 3 km altitudes. The
 223 HAMMONIA data were searched for long-period oscillations up to 110 km. The detailed
 224 analysis is described below (Section 3.2). Nine oscillations were identified with periods
 225 between 5.3 yr and 28.5 yr. They are listed in Table 2a. The oscillation shown in Fig. 1 (17.3
 226 yr) is from about the middle of this range.

226

227

228

229

230

231 2.3 WACCM

232

233 Long runs with chemistry-climate models (CCMs) having restricted boundary conditions
234 are not frequently available. A model run much longer than 34 years became available from
235 the CESM-WACCM4 model. This 150 year run was analyzed from the ground up to 108 km.
236 The model experiments are described in Hansen et al. (2014). Here, the experiment with
237 monthly varying constant climatological SSTs and sea ice has been used, i.e., there is a
238 seasonal variation, but it is the same in all years. Other boundary conditions such as
239 Greenhouse Gases (GHG) and Ozone Depleting Substances (ODP) were kept constant at
240 1960 values.

241 Solar cycle variability, however, was not kept constant during this model experiment.
242 Spectrally resolved solar irradiance variability as well as variations of the total solar
243 irradiance and the F10.7cm solar radio flux were used from 1955 to 2004 from Lean et al.
244 (2005). Thereafter solar variations from 1962-2004 were used as a block of proxy data and
245 added to the data series several times to reach 150 years in total. Details are given in Matthes
246 et al. (2013).

247 The WACCM data were analyzed for **long-period** oscillations in the same manner as the
248 HAMMONIA data. Here, the emphasis is on longer periods. Besides many shorter
249 oscillations, nine oscillations with periods of more than 20 years were found. These results are
250 included to Table 2a.

251

252

253 2.4 ECHAM6

254

255 The longest computer run available to us, covering 400 years, is from ECHAM6. ECHAM6
256 (Stevens et al., 2013) is the successor of ECHAM5, the base model of HAMMONIA. Major
257 changes relative to ECHAM5 include an improved representation of radiative transfer in the
258 solar part of the spectrum, a new description of atmospheric aerosol, and a new representation
259 of the surface albedo. While the standard configuration of ECHAM5 used a model top at 10
260 hPa, this was extended to 0.01 hPa in ECHAM6. As the atmospheric component of the Max-
261 Planck-Institute Earth System Model (MPI-ESM, Giorgetta et al., 2013) it has been used in a
262 large number of model intercomparison studies related to the Coupled Model Intercomparison
263 Project phase 5 (CMIP5). The ECHAM6 simulation analyzed here was run at T63 spectral
264 resolution with 47 vertical layers (not allowing for an internal generation of the QBO). All
265 boundary conditions were fixed to constant values, taken as an average of the years 1979 to
266 2008.

267 The temperature data were analyzed as the other data sets described above. Seventeen
268 oscillation periods longer than 20 yr were obtained (Table 2a). The ECHAM6 results in this
269 paper are considered an approximate extension of the HAMMONIA results.

270

271 A summary of the model properties is given in Table 1. All analyses in this paper are for
272 Central Europe. The vertical model profiles are for 50°N, 7°E.

273

274

275

276

277

278

279

280

281

3 Model results

282
283
284
285
286
287
288
289
290
291
292
293
294
295
296
297
298
299
300
301
302
303
304
305

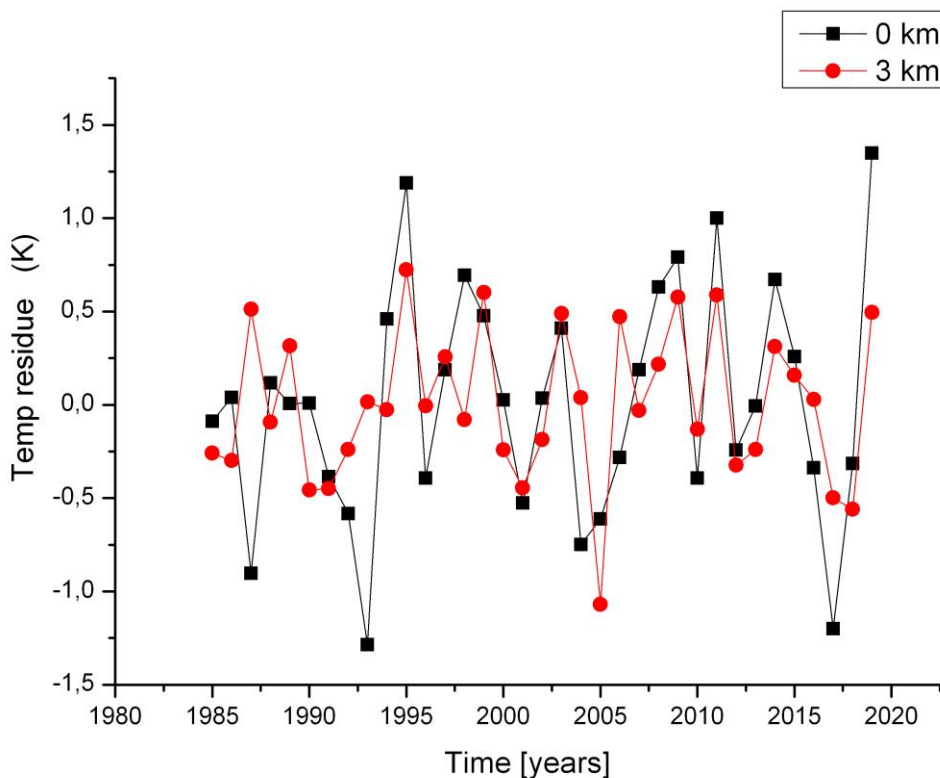
3.1 Vertical correlations of atmospheric temperatures

Figure 1 indicates that there are some vertical correlation structures in the atmospheric temperatures. This was studied in detail for the HAMMONIA and ECHAM6 data.

Ground temperature residues from the HAMMONIA run 38123 (34 years) are shown in Fig. 2 (black squares). The mean temperature is 281.89 K, which was subtracted from the model data. The boundary conditions (sun, ocean, green house gases, soil humidity, land use, vegetation) have been kept constant, as discussed above. The temperature fluctuations thus show the atmospheric variability (standard deviation is $\sigma = 0.62$ K). This variability is frequently termed “(climate) noise” in the literature. It will be checked whether this notion is justified in the present case.

Also shown in Fig. 2 are the corresponding HAMMONIA data for 3 km altitude. The mean temperature is 266.04 K, the standard deviation is $\sigma = 0.41$ K. The statistical error of these two standard deviations is about 12%. Hence the internal variances at the two altitudes are statistically different. This suggests that there may be a vertical structure in the variability that should be analyzed.

The data sets in Fig. 2 show large changes within short times (2-4 years). Sometimes these changes are similar at the two altitudes. The variability of HAMMONIA thus appears to contain an appreciable high frequency component and thus needs to be analyzed as well for vertical as for spectral structures.



306
307
308
309
310

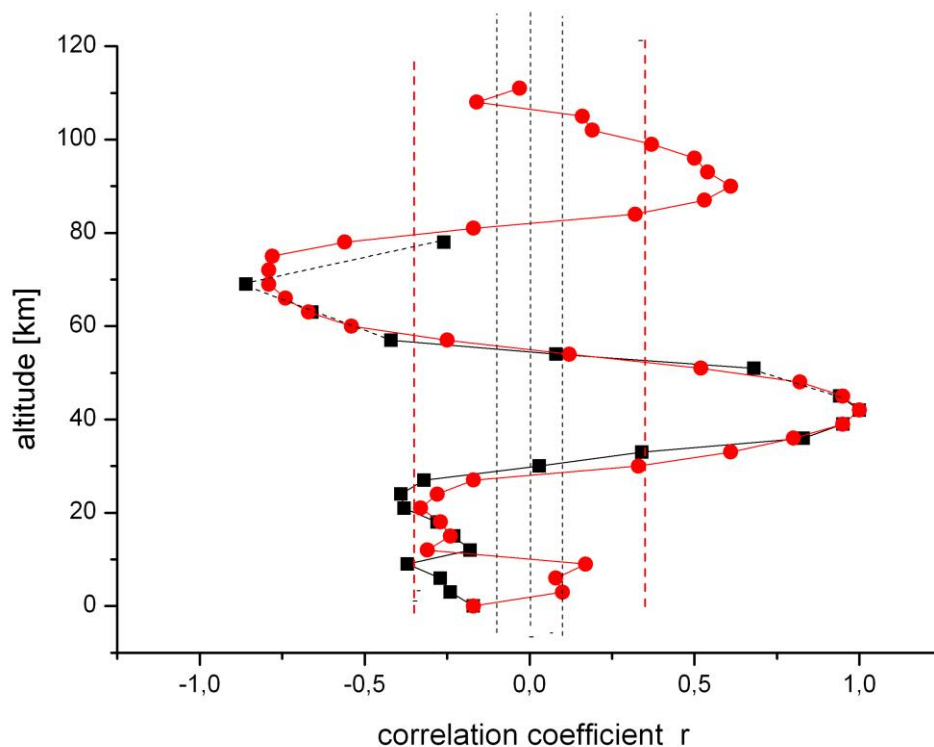
Fig. 2 HAMMONIA temperature residues at 0 km and 3 km altitude with fixed boundary conditions (see text). Mean temperatures of 281.89 K (0 km) and 266.04 K (3 km) have been subtracted from the model temperatures. Data are for 50°N, 7°E.

311
312 Temperatures at layers 3 km apart in altitude were therefore correlated with those at 42 km as
313 a reference altitude (near stratopause). The results are shown in Fig. 3 for the HAMMONIA
314 model run up to 105 km (red dots). A corresponding analysis for the much longer model run
315 of ECHAM6 is also shown (black squares, up to 78 km). Two important results are obtained:
316 1) There is an oscillatory vertical structure in the correlation coefficient r with a maximum in
317 the upper mesosphere/lower thermosphere, and two minima in the lower stratosphere and in
318 the mesosphere, respectively (for HAMMONIA). The correlations are highly significant near
319 the upper three of these extrema (see the 95% lines in Fig. 3). 2) The correlations in the two
320 different data sets are nearly the same above the troposphere. This is remarkable because the
321 two sets cover time intervals very different in length (34 years vs 400 years, respectively).
322 Therefore, the correlation structure appears to be a basic property of the atmosphere (see
323 below).

324 The correlations suggest that the fluctuations in the atmosphere (or part of them) are
325 somehow “synchronized” at adjacent altitude levels. A vertical (layered) structure might
326 therefore be present in the magnitude of the fluctuations, too. This was studied by means of
327 the standard deviations σ of the temperatures T , the result is shown in Fig. 4. There is indeed a
328 vertical structure with fairly pronounced layers.

329 The HAMMONIA data used for Fig. 4 were annual data that have been smoothed by a four
330 point running mean. This was done to reduce the influence of high frequency “noise”
331 mentioned above, which is substantial (a factor of 2). The correlation calculations were
332 repeated with the unsmoothed data. The results are essentially the same. The same applies to
333 the standard deviations.

334 The layered structures shown in Fig. 3 and 4 are not unrelated. This can be seen in Fig. 4
335 that also gives the vertical correlations r (Fig. 3) for comparison. The horizontal dashed lines
336 indicate that the maxima of the standard deviations occur near the extrema of the correlation
337 profile in the stratosphere and lower mesosphere. This suggests that the fluctuations in
338 adjacent σ maxima (and in adjacent layers) are anticorrelated. Surprisingly these
339 anticorrelations are also approximately seen in the amplitude and phase profiles of Fig.1 that
340 are typical of all oscillations (see below).
341



342
343

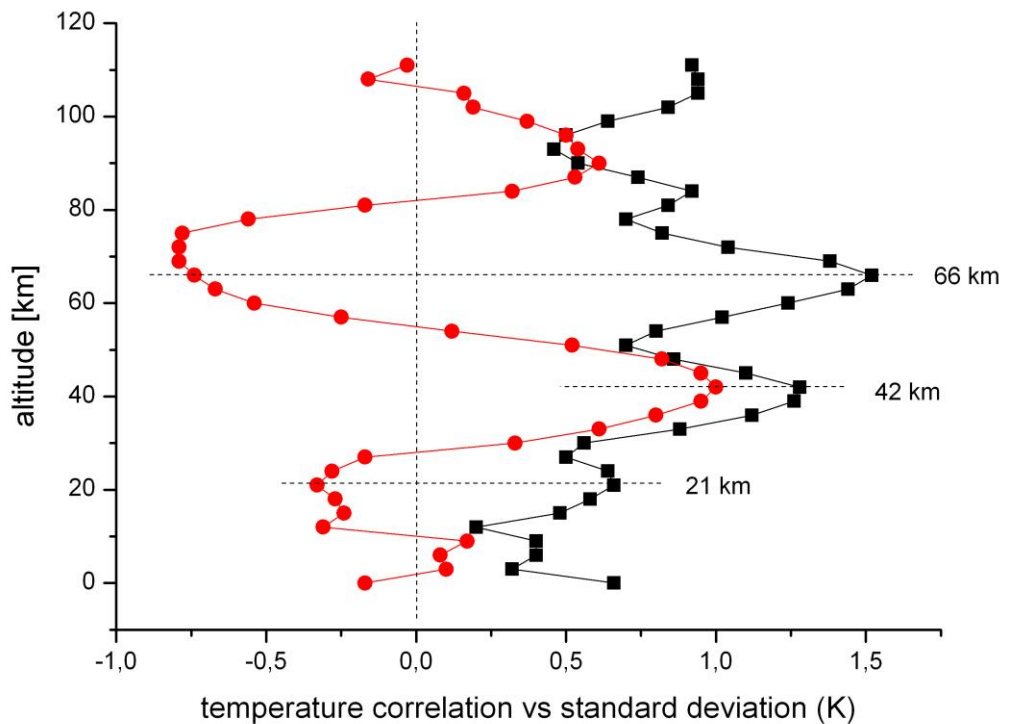
344 Fig. 3 Vertical correlation of temperatures in HAMMONIA (red dots) and ECHAM6 (black
345 squares). Reference altitude is 42 km ($r = 1$). Vertical dashed lines show 95% significance for
346 HAMMONIA (red) and ECHAM6 (black).

347
348

349 The ECHAM6 data have been analyzed in the same way as the HAMMONIA data,
350 including a smoothing by a 4 point running mean. The data cover the altitude range of 0
351 -78 km for a 400 year simulation. The results are very similar to those of
352 HAMMONIA. This is shown in Fig. 5 that gives vertical profiles of standard deviations and
353 of vertical correlations of the smoothed ECHAM6 data, and is to be compared to the
354 HAMMONIA results in Fig. 4. The two upper maxima of standard deviations are again
355 anticorrelated.

356 It is apparently a basic property of the atmosphere's internal variability to be organized in
357 some kind of "layers", and that adjacent layers are anti-correlated. It appears therefore
358 questionable whether the internal variability may be termed "noise", as is frequently done in
359 the literature.

360
361



362
363

364 Fig. 4 HAMMONIA temperatures: Comparison of standard deviations (black squares,
365 multiplied by 2 for easier comparison) and correlation coefficients (red dots, see Fig. 3). For
366 details see text.

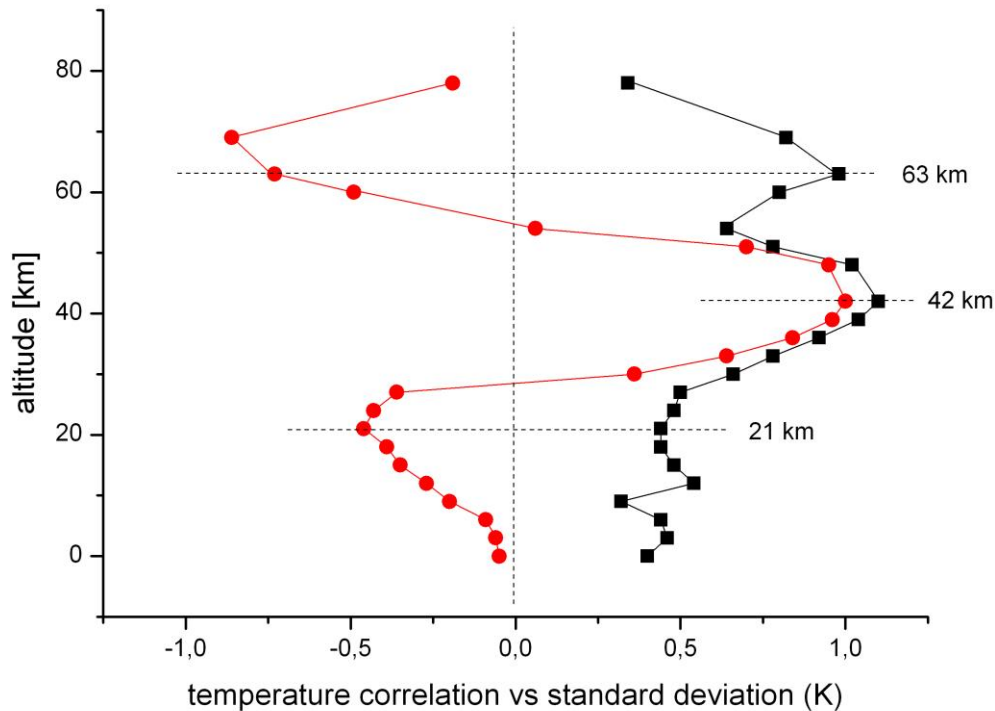
367
368
369

370 3.2 Time structures

371

372 The correlations/anticorrelations concern temporal variations of temperatures. This suggests
373 a search for some kind of regular (ordered) structure in the time series, as well. Therefore in a
374 first step, FFT analyses have been performed for all HAMMONIA altitude levels (3 km
375 apart). The results are shown in Fig. 6 that gives amplitudes for the period range of 4 - 34
376 years versus altitude. Also in this picture, the amplitudes show a layered structure. In addition
377 an ordered structure in the period domain is also indicated. There are increased or high
378 amplitudes near certain period values, for instance at the left and right hand side and in the
379 middle of the picture. A similar result is obtained for the ECHAM6 data shown in Fig. 7 for
380 the longer periods of 10-400 years. The layered structure in altitude is clearly seen, and so are
381 the increased amplitudes near certain period values. Obviously, the computer simulations
382 contain periodic temperature oscillations, the amplitudes of which show a vertically layered
383 order. Because most boundary conditions of the computer runs were kept constant, these
384 oscillations can hardly be excited from the outside. They are therefore interpreted as “self-
385 excited” oscillations, and thus as intrinsic properties of the atmosphere (see, however,
386 Sect.2.2 and 4.1).

387
388
389



390 Fig. 5 ECHAM6 temperatures: Comparison of standard deviations (black squares,
 391 multiplied by 2) and correlation coefficients (red dots). For details see text.
 392
 393
 394

395 The amplitudes shown in Fig. 6 and 7 are relative values, and the resolution of the spectra is
 396 quite limited. Therefore a more detailed analysis is required. For this purpose the Lomb-
 397 Scargle Periodogram (Lomb 1976; Scargle 1982) is used. As an example Fig. 8 shows the
 398 mean Lomb-Scargle Periodogram in the period range 20 – 100 years for the ECHAM6 data.
 399 For this picture Lomb-Scargle spectra were calculated for all ECHAM6 layers separately, and
 400 the mean spectrum of all altitudes was determined. The power of the periodogram gives the
 401 reduction in sum of squares when fitting a sinusoid to the data (Scargle, 1982), i.e. it is
 402 equivalent to a harmonic analysis using least square fitting of sinusoids. The power values are
 403 normalized by the variance of the data to obtain comparability of the layers with different
 404 variance. Quite a number of spectral peaks are seen between 20 and 60 years period. Further
 405 oscillations appear to be present around 100 years and at even longer periods (not shown here
 406 as they are not sufficiently resolved).

407 We compared the mean result for the ECHAM6 data with 10000 representations of noise.
 408 One representation covers 47 atmospheric layers. For each representation we took noise from
 409 a Gaussian distribution for each atmospheric layer independently, and calculated a mean
 410 Lomb-Scargle Periodogram for every representation in the same way as for the ECHAM6
 411 data.

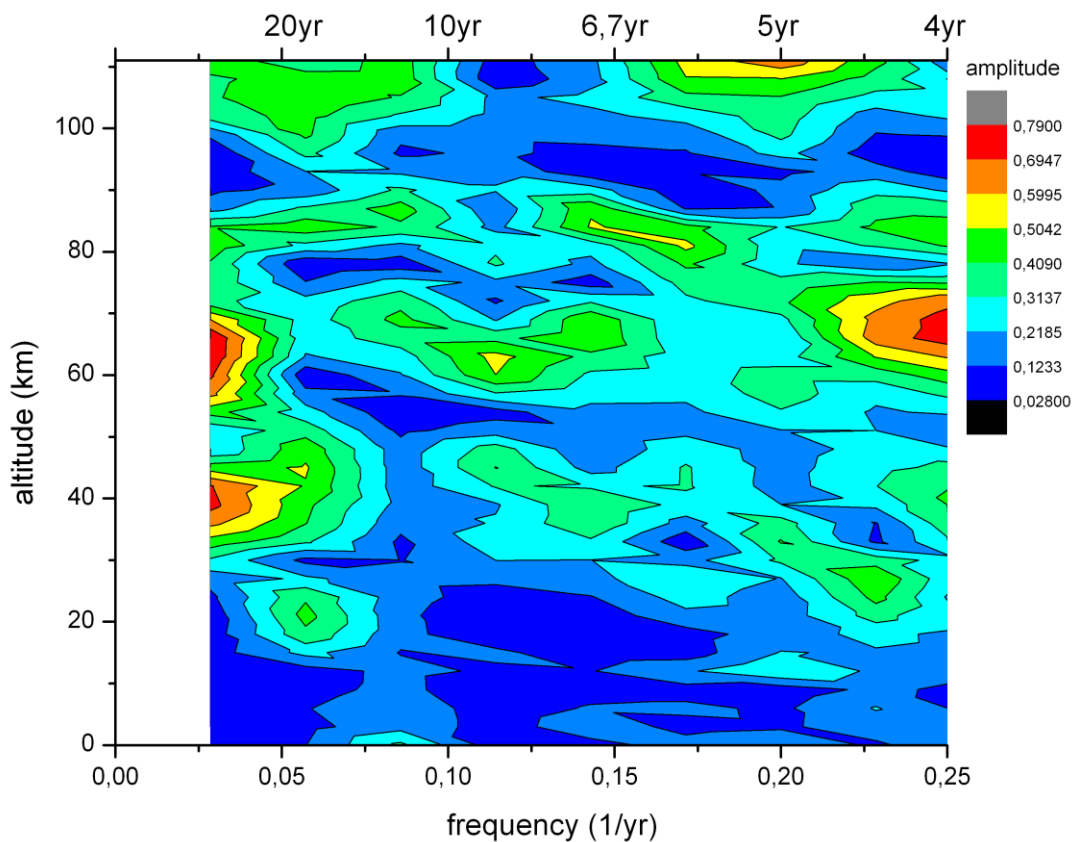
412 It might be considered appropriate to use red noise instead of white noise in this analysis.
 413 We therefore calculated the sample autocorrelation at a lag of 1 year for the different
 414 ECHAM6 altitudes. These values were found to be very close to zero and, thus, we used
 415 Gaussian noise in our analysis.

416 The red line in Fig. 8 shows the average of all of these mean periodograms. As expected for
 417 the average of all representations the peaks cancel, and one gets an approximately constant
 418 value for all periods. A single representation typically shows one or several peaks above this

419 mean level. The red dashed line gives the upper 2σ level, i.e. the mean plus 2σ . As the mean
 420 Lomb-Scargle Periodogram for the ECHAM6 data shows several peaks clearly above this
 421 upper 2σ level, this mean periodogram is significantly different from that of independent
 422 noise. Therefore, the conclusion is that independent noise at the different atmospheric layers
 423 alone cannot explain the observed periodogram showing large remaining peaks after
 424 averaging.

425 The period values shown in Fig. 8 agree with those given for ECHAM6 in Table 2a which
 426 are from the harmonic analysis described next. The agreement is within the error bars given in
 427 Table 2a (except for 24.3).

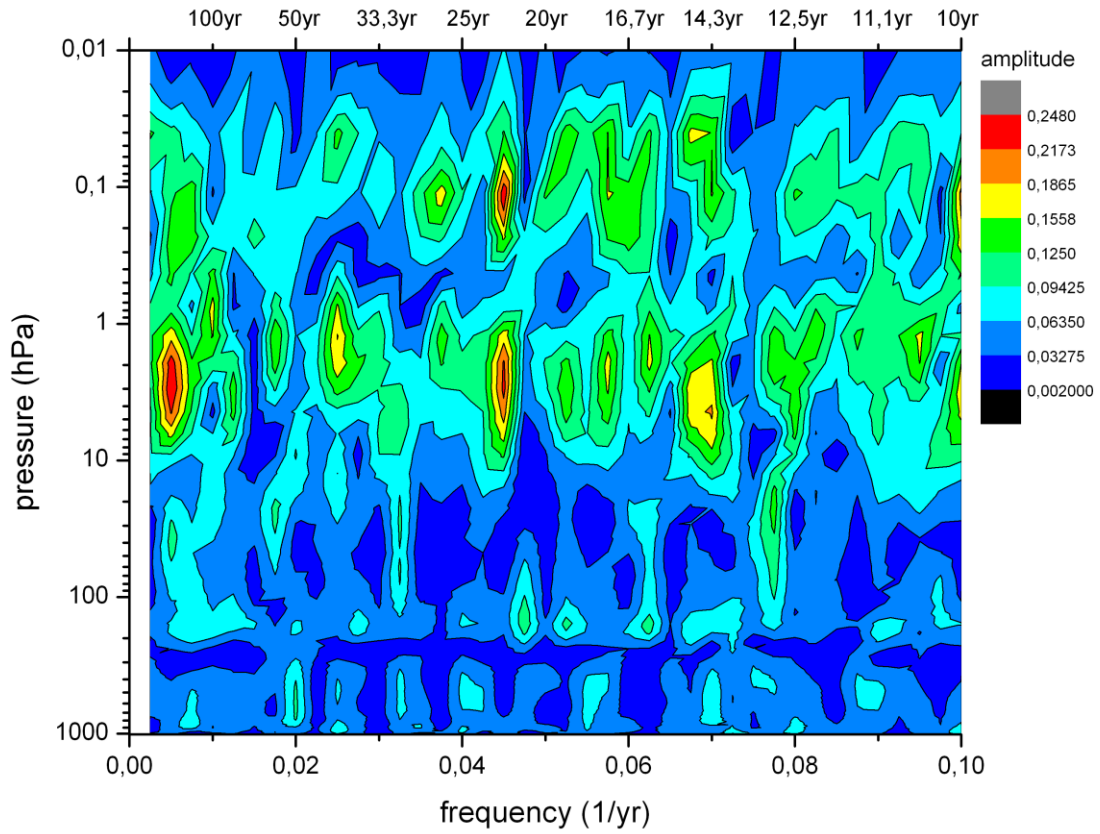
428 A spectral analysis as that in Fig. 8 was also performed for the HAMMONIA temperatures.
 429 It showed the periods of 5.3 yr and 17.3 yr above the 2σ level. These values agree within
 430 single error bars with those given in Table 2a. All peaks found to be significant (in different
 431 analyses) are marked by heavy print in Table 2a.
 432



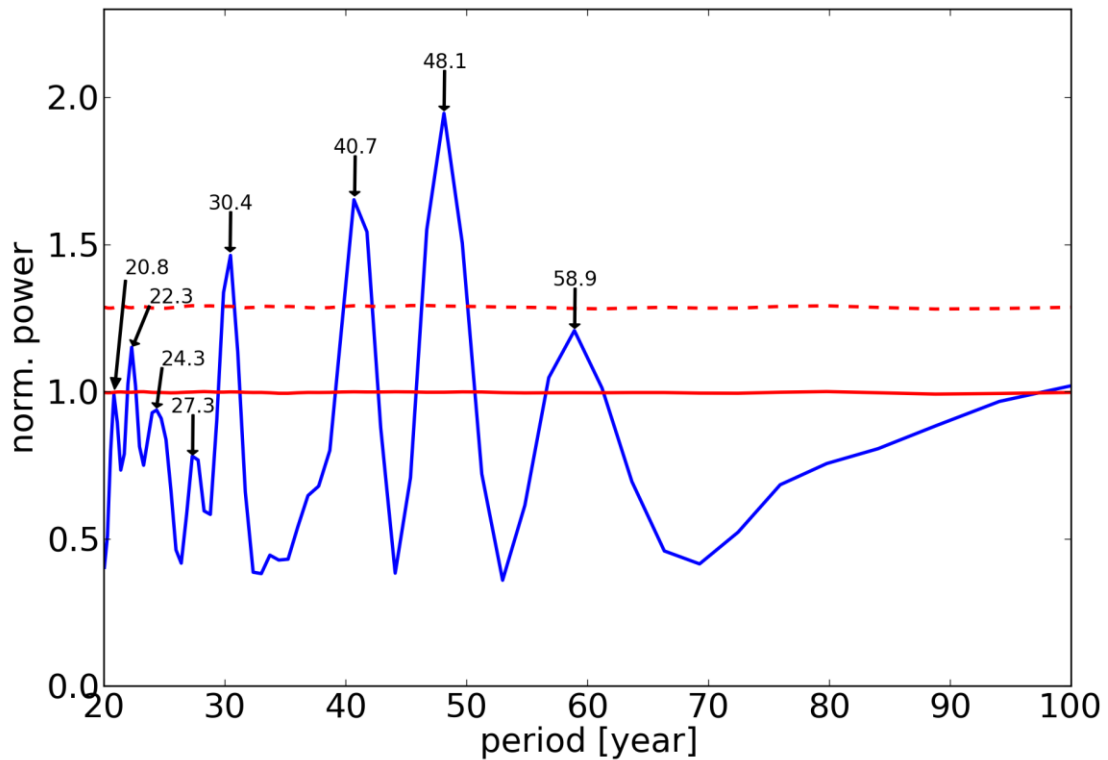
433
 434 **Fig. 6 Long-period** temperature oscillations in the HAMMONIA model.
 435 FFT amplitudes are shown in dependence on altitude and frequency (periods 4 – 34 yr).
 436 Colour code of amplitudes is in arbitrary units.

437
 438
 439 The Lomb-Scargle spectra (in their original form) do not reveal the phases of the
 440 oscillations. We have therefore applied harmonic analyses to our data series. This was done
 441 by stepping through the period domain in steps 10% apart. In each step we looked for the
 442 largest near-by sinus oscillation peak. This was done by means of an ORIGIN search
 443 algorithm (ORIGIN Pro 8G, Levenberg-Marquardt algorithm) that yielded optimum values
 444 for period, amplitude, and phase. The algorithm starts from a given initial period and looks for
 445 a major oscillation in its vicinity. For this it determines period, amplitude, and phase,
 446 including error bars. If in this paper the term “harmonic analysis” is used, this algorithm is
 447 always meant. The results are a first approximation, though, because only one period was

448 fitted at a time, instead of the whole spectrum. Furthermore, the 10% grid may be sometimes
449 too coarse. Also small amplitude oscillations may be overlooked.
450
451
452
453



454
455
456 Fig. 7 Long-period temperature oscillations in the ECHAM6 model.
457 FFT amplitudes are shown in dependence on altitude and frequency (periods 10 – 400 yr).
458 Colour code of amplitudes is in arbitrary units.
459



460
 461
 462
 463
 464

Fig. 8 Long-period temperature oscillations in the ECHAM6 model
 Lomb-Scargle periodogram is given for periods of 20 – 100 years. Dashed red line indicates
 significance at the 2σ level. For straight red line see text.

465

466

467 This analysis was performed for all altitude levels available. Figure 1 shows an example for
 468 the HAMMONIA temperatures from 3-111 km for periods around 15 – 20 years. The middle
 469 track (red dots) shows the periods with their error bars, the left side shows the amplitudes, and
 470 the right side the phases. The mean of all periods is 17.3 ± 0.79 years. There are several
 471 altitudes where the harmonic analysis does not give a period. This may occur if an amplitude
 472 is very small or if there is a near-by period with a strong amplitude that masks the smaller
 473 one. At these altitudes the periods were interpolated for the fit (dash-dotted vertical line). The
 474 mean of the derived periods (17.3 yr) is used as an estimated interpolation value. This is
 475 because the derived periods do not deviate too much from the mean value. This procedure
 476 allows to obtain estimated amplitude and phase values for instance in the vicinity of the
 477 amplitude minima. That is important because at these altitudes large phase changes are
 478 frequently observed. The Levenberg-Marquardt algorithm calculates an amplitude and phase
 479 if a prescribed (estimated) period is provided.

480

481 The right track in Fig. 1 shows the phases of the oscillations. The special feature about this
 482 vertical profile is its steplike structure with almost constant values in some altitudes and a
 483 subsequent fast change somewhat higher to some other constant level. These changes are by
 484 about 180° (π), i.e. the temperatures above and below these levels are anti-correlated. At these
 485 levels the temperature amplitudes (left track) are minimum, with maxima in between. These
 486 maxima occur near the altitudes of the maxima of the temperature standard deviations in Fig.
 4 that are anti-correlated in adjacent layers. The phase steps in Fig. 1 approximately fit to this

487 picture. They suggest that the layer anti-correlation discussed above corresponds at least in
488 part to the phase structure of the **long-period** oscillations in the atmosphere.

489 This important result was checked by an analysis of other oscillations contained in the
490 HAMMONIA data series. Nine oscillations with periods between 5.34 years and 28.5 years
491 were obtained by the analysis procedure described above. They are listed in Table 2a, and all
492 show vertical profiles similarly as in Fig. 1.

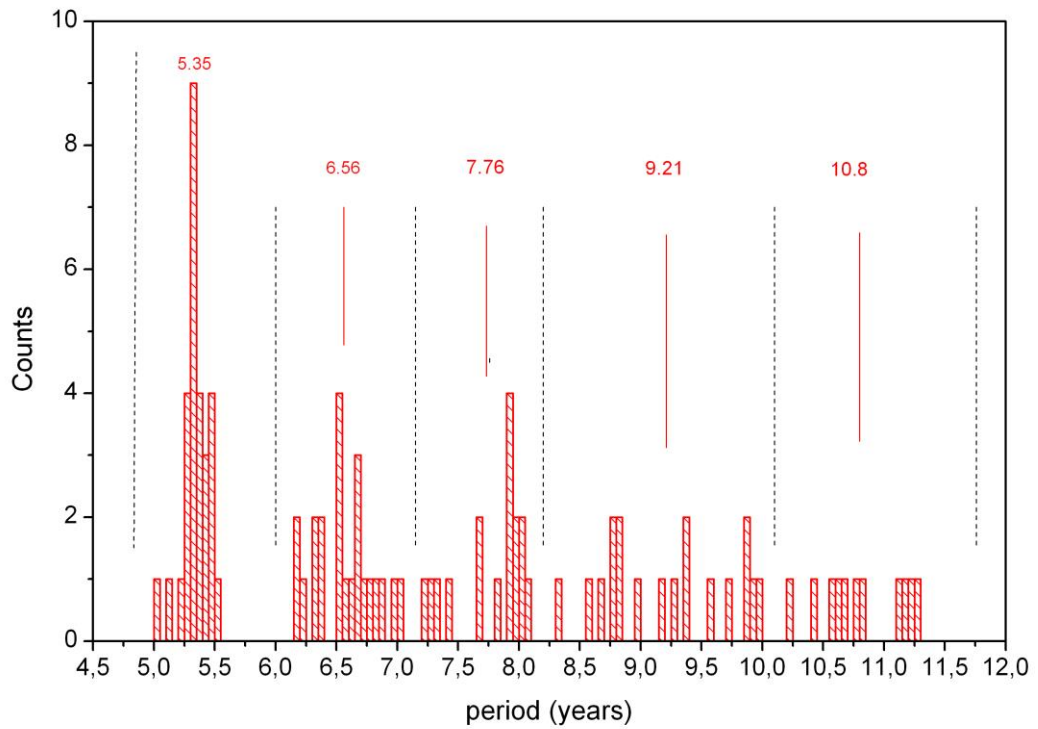
493 Figure 1 shows that at different altitudes the periods are somewhat different. They cluster,
494 however, quite closely about their mean value of 17.3 yr. This clustering about a mean value
495 is found for almost all periods listed in Table 2a. This is shown in detail in Fig. 9 and 10
496 which give the number of periods found at different altitudes in a fixed period interval. The
497 clusters are separated by major gaps, as is indicated by vertical dashed lines (black). This
498 suggests to use a mean period value as an estimate of the oscillation period representative for
499 all altitudes. The mean period values are given above each cluster in red, together with a red
500 solid line. A few clusters are not very pronounced, and hence the corresponding mean
501 period values are unreliable (e.g. those beyond 20 yr, see the increased standard deviations in
502 Table 2a).

503 In determining the mean oscillation periods we have avoided subjective influences as
504 follows: Periods obtained at various altitudes were plotted versus altitude as shown in Fig. 1
505 (middle column, red). When covering the period range 5 to 30 years nine vertical columns
506 appeared. The definition criterion of the columns was that there should not be any overlap
507 between adjacent columns. It turned out that such an attribution was possible. To make this
508 visible we have plotted the histograms in Fig. 9 and 10. The pictures show that the column
509 values form the clusters mentioned which are separated by gaps. The gaps that are the largest
510 ones in the neighbourhood of a peak are used as boundaries (except at 7.15 yr). It turns out
511 that if an oscillation value near to a boundary is tentatively shifted from one cluster to the
512 neighbouring one the mean cluster values experience only minor changes. Figure 10 shows
513 that our procedure comes to its limits, however, for periods longer than 20 years (for
514 HAMMONIA). This is seen in Tab.2a from the large error bars. We still include these values
515 for illustration and completeness.

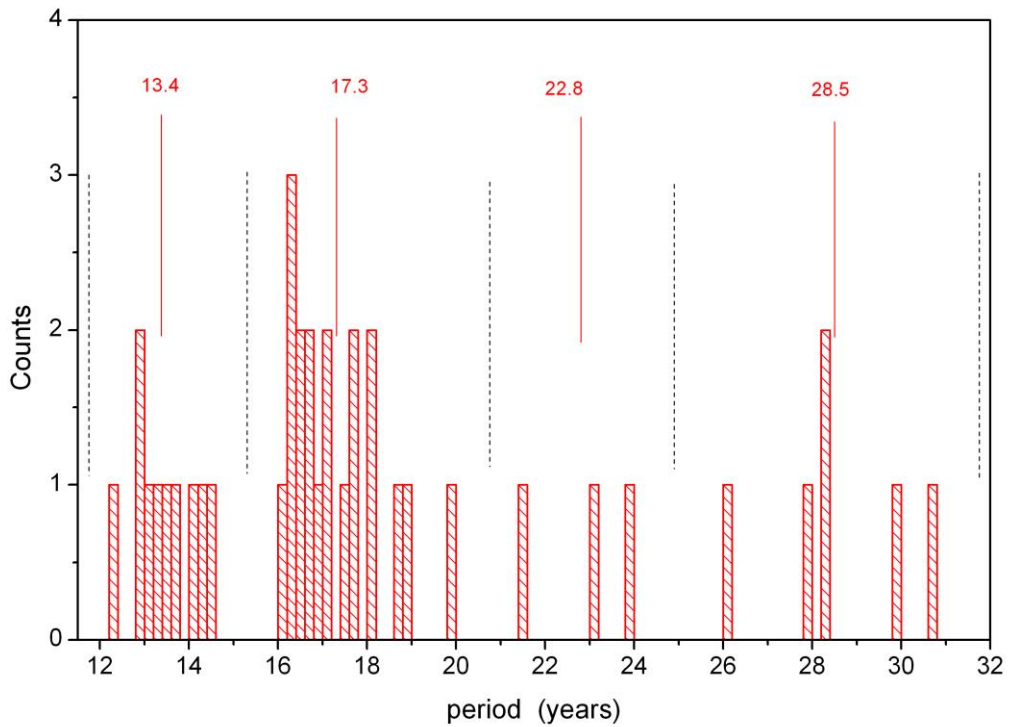
516 It is important to note that all HAMMONIA values in Tab.2a (except 28.5 yr) agree with
517 the Hohenpeißenberg values within the combined error bars. The Hohenpeißenberg data are
518 ground values and hence not subject to our clustering procedure. Furthermore also all other
519 model periods in Tab.2a have been derived by the same cluster procedure. The close
520 agreement discussed in the text suggests that this technique is reliable.

521
522 ECHAM6 - data are used in the present paper to analyze much longer time windows (400
523 years) than that of HAMMONIA (34 years). Results shown in Fig. 3, 5, and 7 are quite
524 similar to those of HAMMONIA. Harmonic analysis of **long** oscillation periods was
525 performed in the same way as for HAMMONIA. Seventeen periods were found longer than
526 20 years and have been included to Table 2a. Shorter periods are not shown here as that range

527 is covered by HAMMONIA. The amplitude and phase structures of these are very similar to



528
529 Fig. 9 Number of oscillations counted in a fixed period interval at periods 4.75 – 11.75
530 years. Interval is 0.05 years. (HAMMONIA)

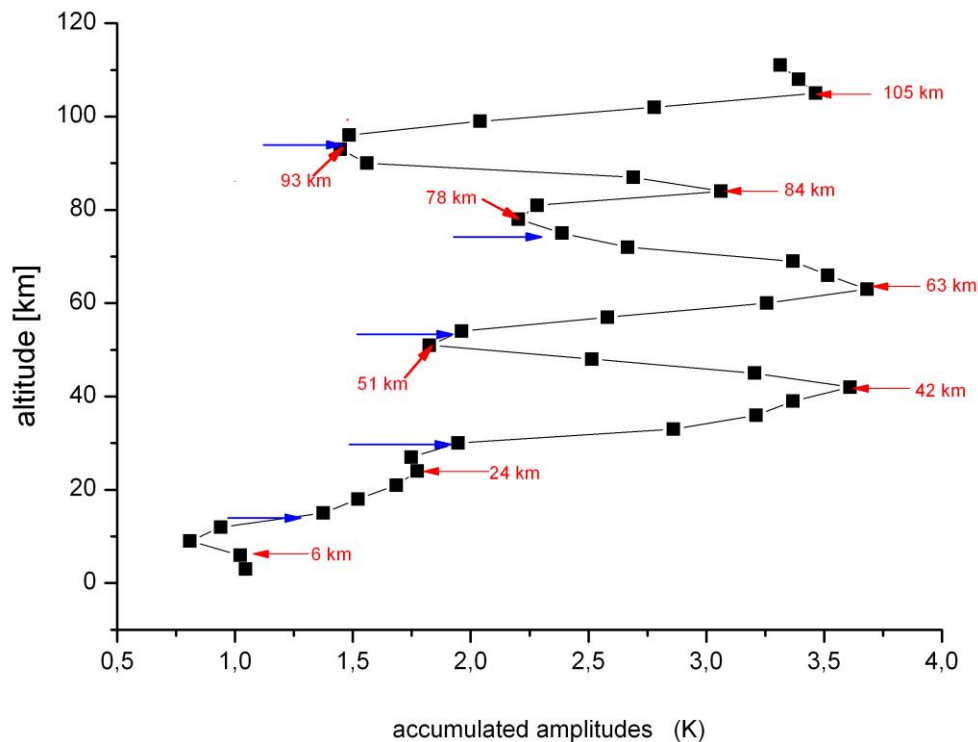


531
532 Fig. 10 Number of oscillations counted in a fixed period interval at periods 11.75 – 31.75
533 years. Interval is 0.2 years. (HAMMONIA)

534 those of HAMMONIA. The cluster formation about the mean period values is also obtained
 535 for ECHAM6 and looks quite similar to Fig. 9 and 10.
 536

537 The vertical amplitude and phase profiles of the mean periods given in Table 2a all show
 538 intermittent amplitude maxima/minima, and step-like phase structures. They in general look
 539 very similar to Fig. 1. We have calculated the accumulated amplitudes (sums) from all of
 540 these profiles at all altitudes. They are shown in Fig. 11a for HAMMONIA. They clearly
 541 show a layered structure similar to the temperature standard deviations in Fig. 4, with maxima
 542 at altitudes close to those of the standard deviation maxima. The figure also closely
 543 corresponds to the amplitude distribution shown in Fig. 1, with maxima and minima occurring
 544 at similar altitudes in either picture.

545 Accumulated amplitudes have also been calculated for the ECHAM6 periods, and similar
 546 results are obtained as for HAMMONIA (see Fig. 11b). The similarity is already indicated in
 547 Fig. 3 above 15 km. The correlation of the HAMMONIA and ECHAM6 curves above this
 548 altitude has a correlation coefficient of 0.97. This and Fig. 11 support the **idea that all of our**
 549 **long-period oscillations** have a similar vertical amplitude structure.



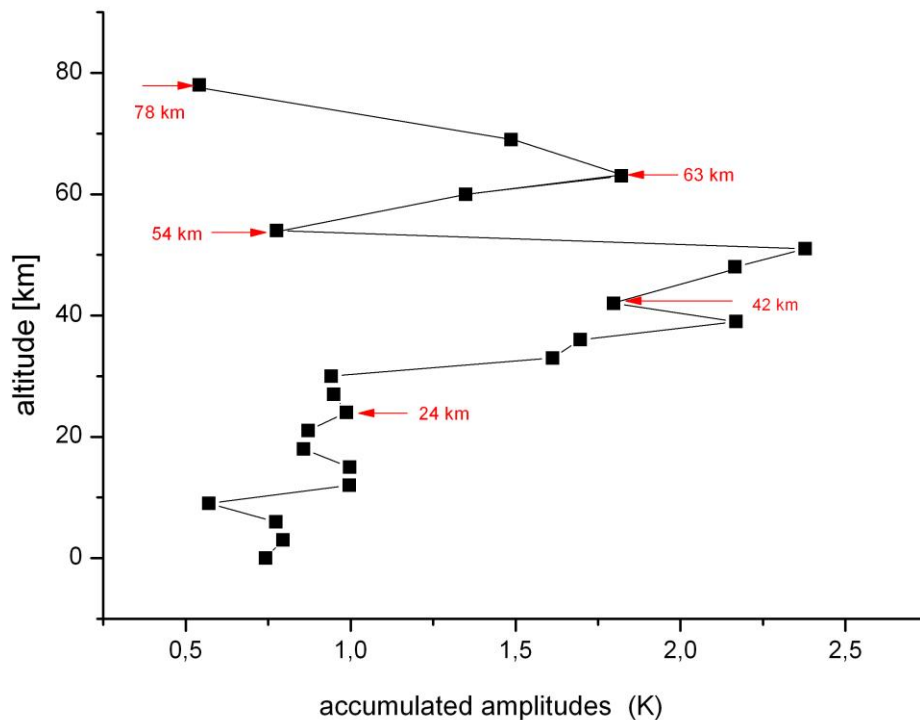
550
 551
 552 Fig. 11a **Long-period** temperature oscillations in the HAMMONIA model.
 553 Accumulated amplitudes are shown vs altitude for periods of 5.3 – 28.5 years (see Table 2a).
 554 Blue horizontal arrows show mean altitudes of phase jumps. Red arrows indicate altitudes of
 555 maxima and minima.
 556

557
 558 The phase jumps in the nine oscillation vertical profiles of HAMMONIA also occur at
 559 similar altitudes. Therefore the mean altitudes of these jumps have been calculated and are
 560 shown in Fig. 11a as blue horizontal arrows. They are seen to be close to the minima of the
 561 accumulated amplitudes and thus confirm the anticorrelations between adjacent layers.
 562 Figures 4, 1, and 11 thus show a general structure of temperature correlations/anticorrelations

563 between different layers of the HAMMONIA atmosphere, and suggest the phase structure of
 564 the oscillations as an explanation. The same is valid for ECHAM6.

565 Altogether HAMMONIA and ECHAM6 consistently show the same type of variability and
 566 oscillation structures. This type occurs in a wide time domain of 400 years. As mentioned, we
 567 do not believe that these ordered structures are adequately described by the term “noise”, as
 568 this notion is normally used for something occurring at random.

569
 570
 571
 572



573
 574

575 Fig. 11b Long-period temperature oscillations in the ECHAM6 model
 576 Accumulated amplitudes are shown vs altitude for the periods given in Tab. 2a. Red arrows
 577 indicate altitudes of maxima and minima.

578

579

580 3.3 Intrinsic oscillation periods

581

582 Three different model runs of different lengths have been investigated by the harmonic
 583 analysis described. The HAMMONIA model covered 34 years, the WACCM model covered
 584 150 years, and the ECHAM6 model covered 400 years. The intention was to study the
 585 differences resulting from the different nature of the models, and from the difference in the
 586 length of the model runs.

587 The oscillation periods found in these model runs are listed in Table 2a. These periods are
 588 vertical mean values as described for Fig. 1 and Figs. 9-10. Periods are given in order of
 589 increasing values in years together with their standard deviations. Only periods longer than 5
 590 years are shown here. The maximum period cannot be longer than the length of the computer
 591 run. Therefore, the number of periods to be found in a model run can -in principle- be the

592 larger the longer the length of the run is. Table 2a shows preferentially periods longer than 20
593 yr (except for HAMMONIA and Hohenpeißenberg) as the emphasis is on the long periods
594 here. Periods comparable to the length of the data series need, of course, be considered with
595 caution.

596 The periods shown here at a given altitude are from the Levenberg-Marquardt algorithm (at
597 1σ significance). The values obtained at different altitudes in a given model have been
598 averaged as described above, and the corresponding mean and its standard error is given in
599 Tab.2a.

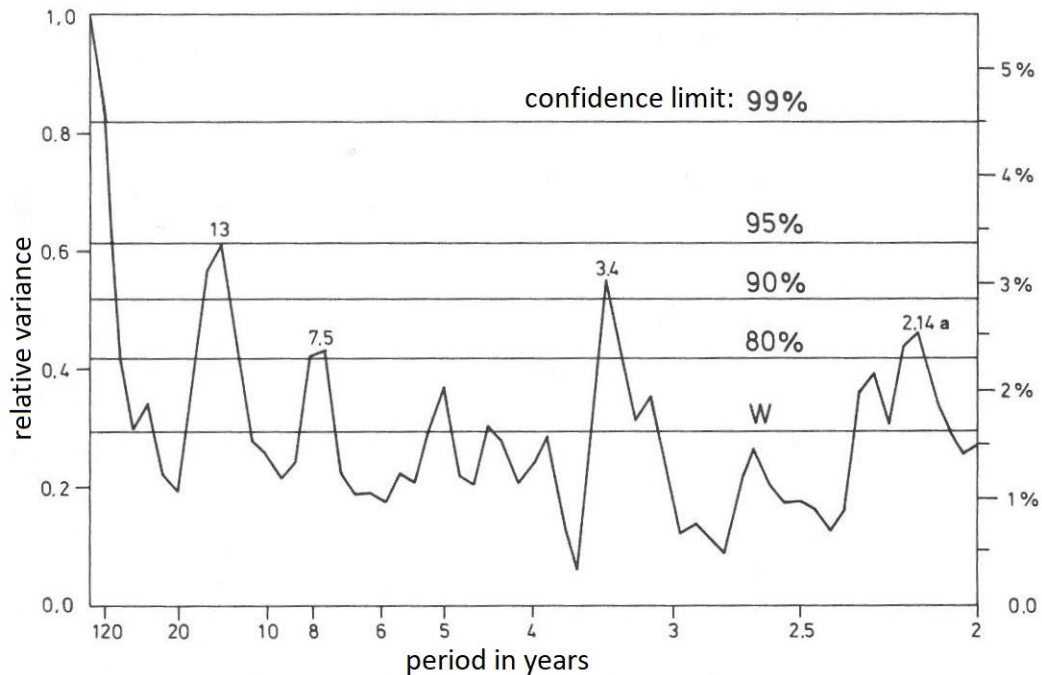
600 Table 2a also contains two columns of periods and their standard deviations that were
601 derived from *measured* temperatures. These are data obtained on the ground at the
602 Hohenpeißenberg Observatory (47.8°N, 11.0°E) from 1783 to 1980, and globally averaged
603 GLOTI data (Global Land Ocean Temperature Index , Hansen et al., 2010), respectively. The
604 data are annual mean values smoothed by a 16 point running mean and will be discussed
605 below. Data after 1980 are not included in the harmonic analyses because they steeply
606 increase thereafter (“climate change”). The periods are determined as for the data of the other
607 rows of Table 2a (see Section 3.2).

608 The Hohenpeißenberg and GLOTI periods show several close agreements with the
609 HAMMONIA and ECHAM6 results. Further comparisons with other data analyses are given
610 below. A summary is given in Table 2b. Different techniques have been used, such as Single
611 Spectrum Analysis (SSA), Auto correlation Spectral Analysis (ASA), and Detrended
612 Fluctuation Analysis (DFA), and yield similar results. They are also shown in Tab. 2b. For the
613 accuracy and significance of these techniques the reader is referred to the corresponding
614 papers. The periods listed in Tab. 2b are given in bold type in Tab.2a.

615 There are some empty spaces in the lists of Table 2a. It is believed that this is because these
616 oscillations are not excited in that model run, or that their excitation is not strong enough to be
617 detected, or that the spectral resolution of the data series is insufficient (strong changes in
618 amplitudes strengths are, for instance, seen in Fig. 1.). For the *measured* data in Table 2a it
619 needs to be kept in mind that they were under the influence of varying boundary conditions.

620 The model runs shown in Table 2a have different altitude resolutions. The best resolution (1
621 km) is available in HAMMONIA (119 vertical layers, run Hhi-max in the earlier paper of
622 Offermann et al., 2015). The very long run of ECHAM6 uses only 47 layers. Data on a 3 km
623 altitude grid are used here. In the earlier paper it was shown on the basis of a limited data set
624 (HAMMONIA, Hlo-max) that a decrease of the number of layers affected the vertical
625 amplitude and phase profiles of the oscillations found. It did, however, not change the
626 oscillation periods. For a more detailed analysis a 20 year-long run of Hlo-max (67 layers) is
627 now compared to the 34 year- long run of Hhi-max (119 layers). The resulting oscillation
628 periods are shown in Table 3 (together with their standard deviations). Sixteen pairs of
629 periods are listed that all agree within the single error bars (except No. 4). Hence it is
630 confirmed that the periods of the oscillations are quite robust with respect to changes in
631 altitude resolution. The periods of the ECHAM6 run can therefore be considered as reliable,
632 despite their limited altitude resolution.

633
634
635
636



637
 638 Fig. 12 Periodogram (2 yr to 120 yr) of measured Hohenpeißenberg temperatures from
 639 Schönwiese (1992, Abb. 57). Results are from an autocorrelation spectral analysis ASA.
 640
 641

642 When comparing the periods in Table 2a to each other several surprising agreements are
 643 observed. It turns out that all periods of the HAMMONIA and WACCM models find a
 644 counterpart in the ECHAM6 data (not vice versa). These data pairs always agree within their
 645 combined error bars, and mostly even within single error bars. The difference between the
 646 members of a pair is much smaller than the distance to any neighbouring value with higher or
 647 lower ordering number in Table 2a. From this it is concluded that the different models find
 648 the same oscillations. The periods of them are obviously quite robust. This and the fact that
 649 most boundary conditions have been kept constant makes us **suppose** that these oscillations
 650 are “self-excited” (intrinsic) oscillations.

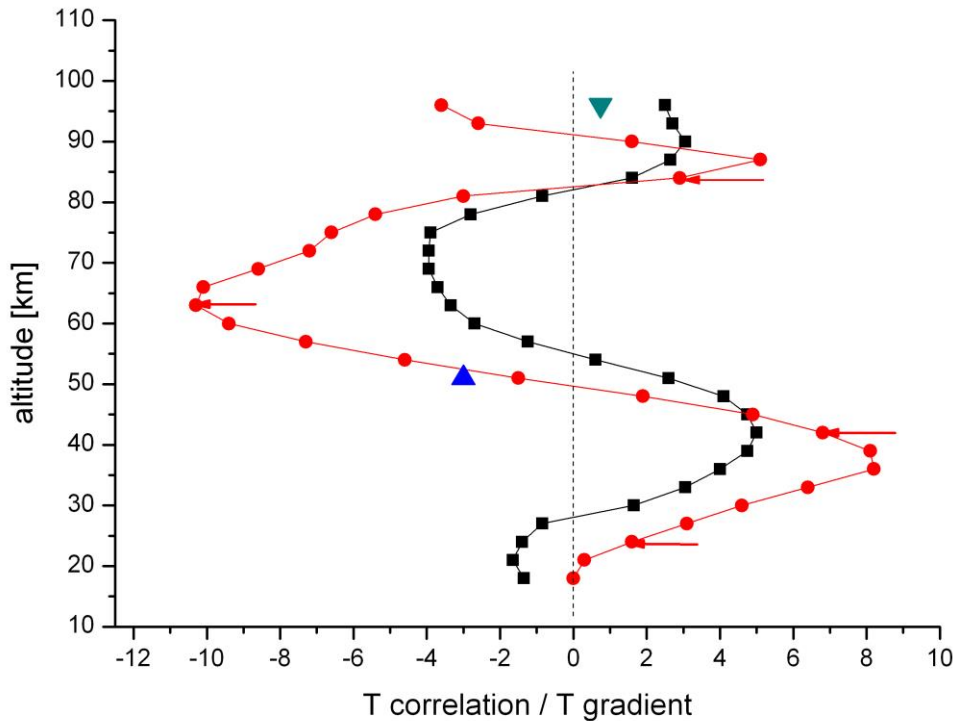
651 A similar agreement is seen for the periods found in the measured Hohenpeißenberg data,
 652 although these have been under the influence of variations of the sun, ocean, and greenhouse
 653 gases. A spectral analysis (auto correlation spectral analysis ASA) of these data is shown in
 654 Fig. 12. It was taken from Schönwiese (1992). The important peak at 3.4 years is not
 655 contained in Table 2, but was found in Offermann et al. (2015). The two peaks near 7.5 yr and
 656 13 yr are close to the values 7.76 ± 0.29 yr and 13.4 ± 0.68 yr in Table 2a.

657 A 335 year long data set of Central England Temperatures (CET) is the longest measured
 658 temperature series available (Plaut et al., 1995). A singular spectrum analysis was applied by
 659 these authors for interannual and interdecadal periods. Periods of 25.0 yr, 14.2 yr, 7.7 yr, and
 660 5.2 yr were identified. All of these values nearly agree with numbers given for HAMMONIA,
 661 WACCM, and/or ECHAM6 in Table 2a (within the error bars given in the Table).

662 Meyer and Kantz (2019) recently studied the data from a large number of European stations
 663 by the method of detrended fluctuation analysis. They identified a period of 7.6 ± 1.8 yr, which
 664 again is in agreement with the HAMMONIA results given in Table 2a (and also agrees with
 665 Fig. 12, and with Plaut et al., 1995).

666 Also the GLOTI data in Table 2a are in agreement with some of the other periods, even
 667 though they are global averages. The results altogether suggest that the periods discussed are
 668 basic (intrinsic) properties of the atmosphere. It will be shown below that they are not limited
 669 to atmospheric temperatures alone, but are, for instance, also seen in Methane mixing ratios.
 670

671
672
673



674
675
676

Fig. 13 Comparison of HAMMONIA vertical correlations from Fig. 3 (black squares) with vertical temperature gradients (red dots). Data are from annual mean temperatures. Correlation coefficients are multiplied by 5. Temperature gradients are approximated by the differences of consecutive temperatures (K per 3 km). Two gradients are given for monthly mean temperature curves in addition: blue triangle for January, green inverted triangle for July. Red arrows show the altitudes of the maxima of the accumulated amplitudes in Fig. 11a.

683
684

3.4 Oscillation amplitudes

685

In an attempt to learn more about the nature of the long period oscillations we analyze their oscillation amplitudes. The determination of absolute amplitudes of self-excited oscillations is difficult and beyond the scope of the present paper. Nevertheless, interesting results can be obtained from their relative values. One of these results is related to the vertical gradients of the atmospheric temperature profiles.

The HAMMONIA model simulates the atmospheric structure as a whole. The annual mean vertical profile of HAMMONIA temperatures can be derived and is seen to vary between a minimum at the tropopause, a maximum at the stratopause, and another minimum near the mesopause (not shown here). In consequence the vertical temperature gradients change from positive to negative, and to positive again. This is shown in Fig. 13 (red dots) between 18 km and 96 km. The temperature gradients are approximated by the temperature differences of consecutive levels.

699 Also shown in Fig. 13 is the correlation profile of HAMMONIA from Fig. 3 (black squares
700 here). The two curves are surprisingly similar. The similarity suggests some connection of the
701 oscillation structure and the mean thermal structure of the middle atmosphere. This is shown
702 more clearly by the accumulated amplitudes of the **long-period** oscillations in Fig. 11a. The
703 maxima of these occur at altitudes near to the extrema of the temperature gradients as is
704 shown by the red arrows in Fig. 13. The mechanism connecting the oscillations and the
705 thermal structure appears to be active throughout the whole altitude range shown (except the
706 lowest altitudes).

707 A possible mechanism might be a vertical displacement of air parcels. If an air column is
708 displaced vertically by some distance D (“displacement height”) a seeming change in mixing
709 ratio is observed at a given altitude. This is a relative change, only, not a photochemical one.
710 It can be estimated by the product $\{D \text{ times mixing ratio gradient}\}$. If the vertical movement
711 is an oscillation, the trace gas variation is an oscillation as well, assuming that D is a constant.
712 Such transports may be best studied by means of a trace gas like CH_4 .

713 HAMMONIA methane mixing ratios have therefore been investigated for oscillation
714 periods in the same way as described above for the temperatures. Results are briefly
715 summarized here.

716 Ten periods have been found, indeed, between 3.56 and 16.75 years by harmonic analyses
717 and are shown in Tab. 3. These periods are very similar to those obtained for the temperatures
718 in Table 2a and 3. The agreement is within the single error bars. Hence it is concluded that the
719 same oscillations are seen in HAMMONIA temperatures and CH_4 mixing ratios.

720 The CH_4 oscillations support the idea that a displacement mechanism is active. The
721 corresponding displacement heights D were estimated from the CH_4 amplitudes and the
722 vertical gradients of the mean HAMMONIA CH_4 mixing ratios.

723 The values D obtained from the different oscillation periods are about the same, though they
724 show some scatter. This makes us presume that the displacement mechanism may be the same
725 for all oscillations. However, D appears to follow a trend in the vertical direction. The
726 displacements are below 100 m in the lower stratosphere and slowly increase with height to
727 above 200 m.

728 Thus the important result is obtained that the **our long-period** oscillations are related to a
729 vertical displacement mechanism that is altitude dependent, but appears to be the same for all
730 periods. A more detailed analysis is beyond the scope of this paper.

731

732

733 3.5 Seasonal aspects

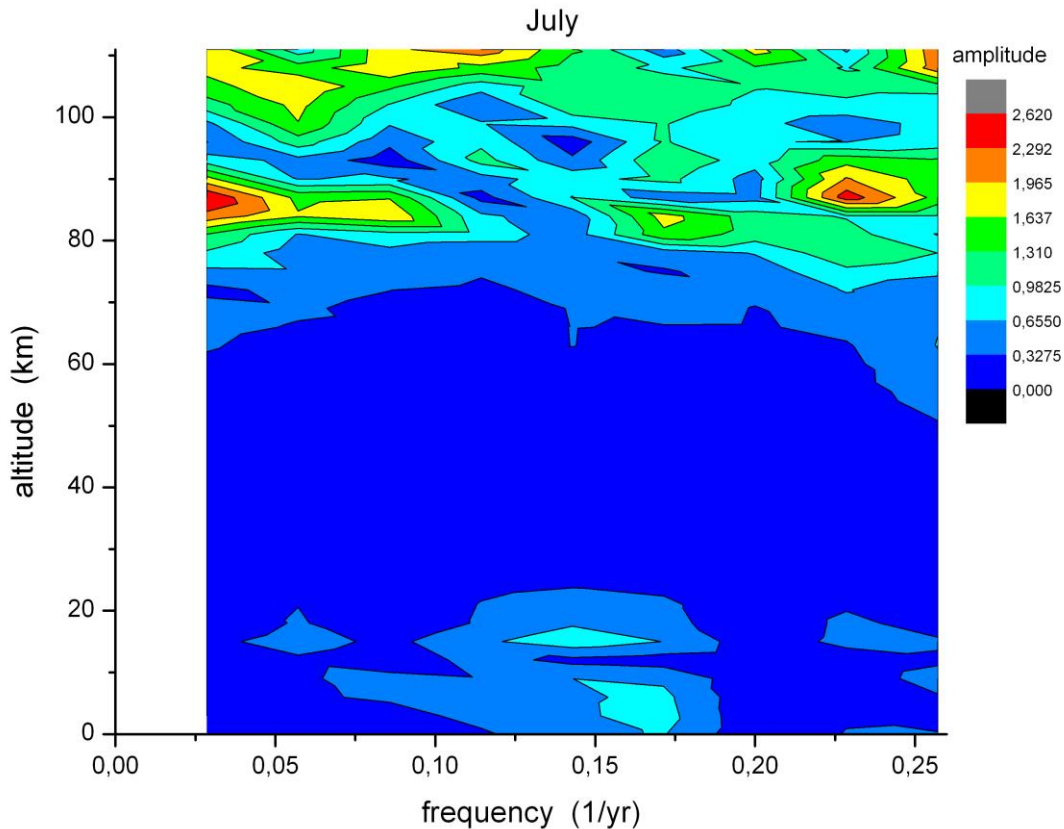
734

735 Our analysis has so far been restricted to annual mean values. Large temperature variations
736 on much shorter time scales are also known to occur in the atmosphere, including vertical
737 correlations (e.g. seasonal variations). This suggests the question whether these might be
738 somehow related to the long period oscillations. Our spectral analysis is therefore repeated
739 using monthly mean temperatures of HAMMONIA.

740 Results are shown in Fig. 14 and 15, which give the amplitude distribution vs period and
741 altitude of FFT analyses for the months of July and January. These two months are typical of
742 summer (May-August), and winter (November-March), respectively. In July oscillation
743 amplitudes are seen essentially at altitudes above about 80 km, and some below about 20 km.
744 In the regime in between, oscillations are obviously very small or not excited. The opposite
745 behaviour is seen in January: oscillation amplitudes are now observed in the middle altitude
746 regime where they had been absent in July. This is to be compared to Fig. 6 and 11 that give
747 the annual mean picture. In Fig. 11 the structures (two peaks) above 80 km appear to
748 represent the summer months (Fig. 14). The structures between 80 km and 30 km, on the
749 other hand, apparently are representative of the winter months (Fig. 15).

750 The monthly oscillations appear to be related to the wind field of the HAMMONIA model.
 751 Figure 16 shows the monthly zonal winds of HAMMONIA from the ground up to 111 km
 752 (50°N). Comparison with Fig. 14 and 15 shows that oscillation amplitudes are obviously not
 753 observed in an easterly wind regime. Hence, the long period oscillations and their phase
 754 changes are apparently related to the dynamical structure of the middle atmosphere. A change
 755 from high to low oscillation activity in the vertical direction appears to be related to a wind
 756 reversal.

757 This correspondence does not, however, exist in all details. In the regimes of oscillation
 758 activity there are substructures. For instance in the middle of the July regime of amplitudes
 759 above 80 km there is a “valley” of low values at about 95 km. A similar valley is seen in the



760 Fig. 14 Long-period temperature oscillations in the month of July in HAMMONIA.
 761 Amplitudes are shown in dependence of altitude and frequency (periods 3.9-34 yr). Colour
 762 code of amplitudes is in arbitrary units.
 763

764
 765
 766 January data around 55 km. Near these altitudes there are phase changes of about 180° (see
 767 the blue arrows in Fig. 11a). Contrary to our expectation sketched above, these are altitudes of
 768 large westerly zonal wind speeds without much vertical change (see Fig.16). However, the
 769 two “valleys” are relatively close to altitudes where the vertical temperature gradients are
 770 small (see Fig. 13). As the gradients from the annual mean temperatures used for the curves in
 771 Fig. 13 may differ somewhat from the corresponding monthly values two monthly gradients
 772 have been added in Fig. 13 for January (at 51 km) and at 96 km (for July). They are small,
 773 indeed, and could explain low oscillation amplitudes by the above discussed vertical
 774 displacement mechanism.

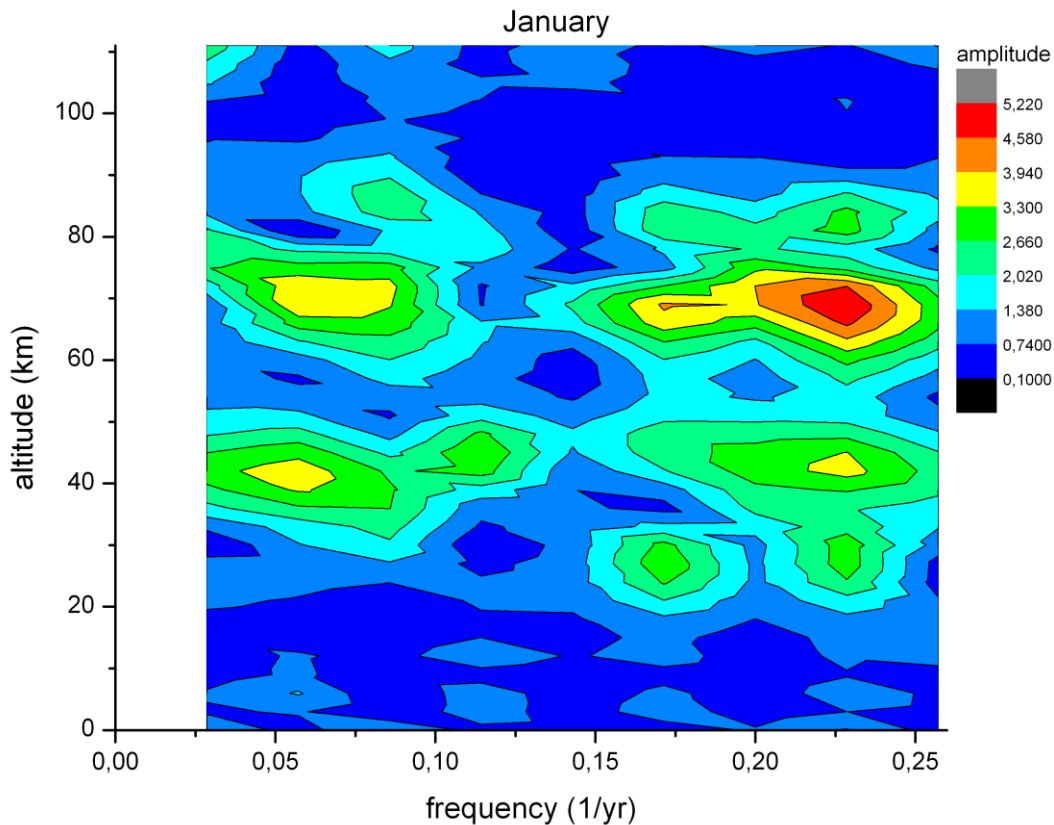
775
 776
 777
 778

779
780
781
782
783
784
785
786
787
788
789
790
791
792
793
794
795
796
797
798

3.6 Oscillation persistence

If our concept of self-excitation of oscillations **were** correct we might expect that such oscillations might also dissipate after a while, i.e. we should expect some intermittence in our oscillation amplitudes. To check on this we have subdivided the 400 years data record of ECHAM6 in four smaller time intervals (blocks) of 100 years each. In each block we performed harmonic analyses for periods of 24 yr (frequency 0.042/yr) and 37 yr (frequency 0.027/yr), respectively, at the altitudes of 42 km (1.9 hPa) and 63 km (0.11 hPa), respectively. These are altitudes and periods with strong signals as seen in Fig. 7. Results for the two altitudes and two periods are given in Fig. 17.

The results show two groups of amplitudes: one is around 0.15 K, the other is very small and compatible with zero. The two groups are significantly different as is seen from the error bars. This result is compatible with the picture of oscillations being excited and not-excited (dissipated) at different times. The non-excitation (dissipation) for the 24 yr oscillation (black squares) occurs in the first block (century), that for the 37 yr oscillation (red dots) in the second block. The 24 yr profile at 63 km altitude is similar as that at 24 km. Likewise, the 37 yr profile at 24 km is similar to that at 63 km. Hence it appears that the whole atmosphere (or a large part of it) is excited (or dissipated) simultaneously. (The two profiles in Fig. 17 appear to be somehow anticorrelated for some reason that is unknown as yet.)



799
800
801
802
803
804
805
806
807

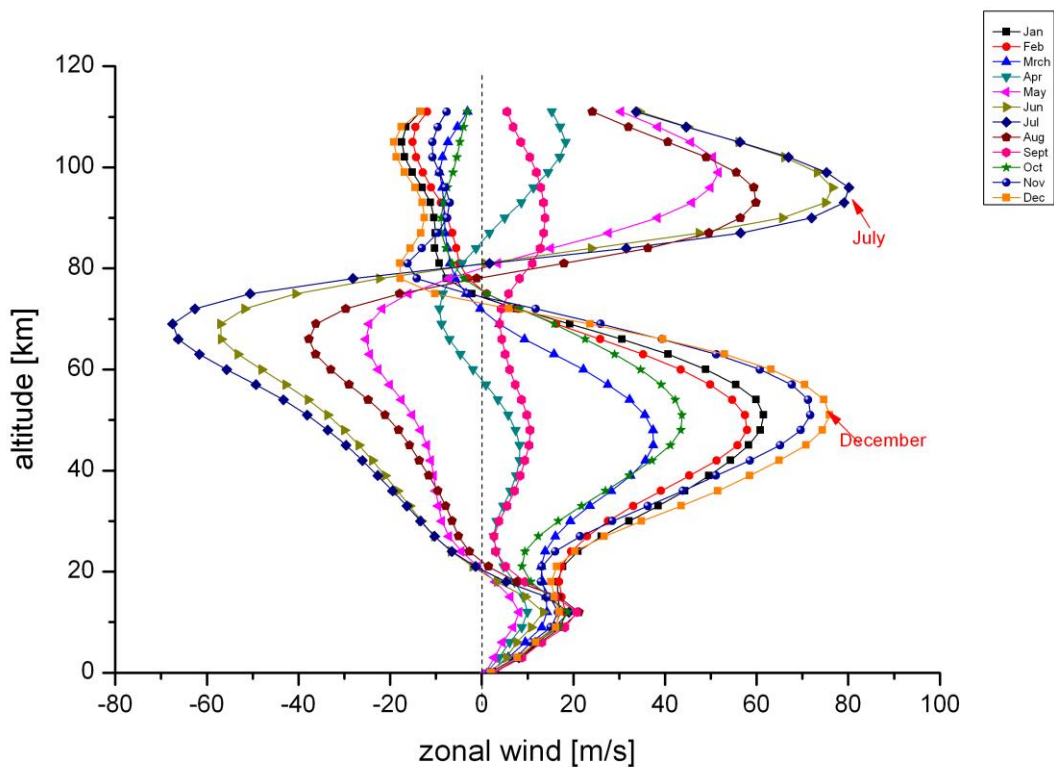
Fig. 15 **Long-period** temperature oscillations as in Fig. 14, but for the month of January

For the analysis of shorter periods the 400 year data set of ECHAM6 may be subdivided in a larger number of time intervals. Figure 18 shows the results for periods of 5.4 yr and 16 yr, respectively, for various altitudes. An FFT analysis was performed in 12 equal time intervals (blocks of 32 yr length) in the altitude regime 0.01 – 1000 hPa and the period regime 4 – 40 yr. The corresponding 12 maps look similar as Fig. 15, i.e. there are pronounced amplitude

808 hot spots at various altitudes and periods. (Of course, the values near the 40 yr boundary are
 809 not really meaningful.) In subsequent blocks these hot spots may shift somewhat in altitude
 810 and/or period, and hence the profiles taken at a fixed period and altitude as those of Fig. 18
 811 show some scatter. Nevertheless, there is strong indication of the occurrence of coordinated
 812 high maxima and deep minima of amplitudes in Blocks 3/ 4 and Blocks 10/11, respectively.
 813 These maxima are interpreted as strong oscillation excitation, whereas the minima are
 814 believed to show (at least in part) the dissipation of the oscillations.

815 It should be mentioned that in the FFT analysis the 5.4 yr period is an overtone of the 16 yr
 816 period. Hence the two period data in Fig.18 may be somehow related.

817
 818
 819
 820



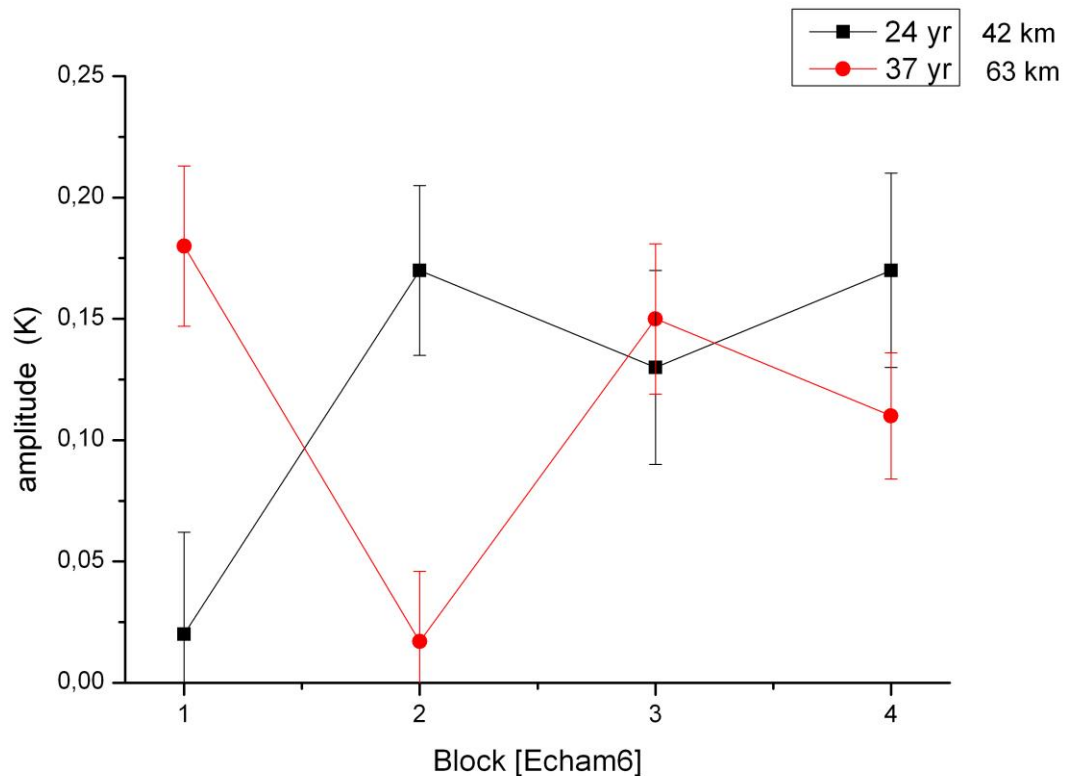
821
 822 Fig. 16 Vertical distribution of zonal wind speed in the HAMMONIA model.
 823

824
 825
 826 4 Discussion
 827

828 4.1 The nature and origin of **our long-period** oscillations are as yet unknown. We
 829 therefore collect here as many of their properties as possible. They do exist in
 830 computer models even if the model boundaries for the influences of the sun, the
 831 ocean, the green house gases are kept constant. Therefore they are **supposed** to be
 832 self-generated oscillations. **However, as said in Section 2.2, some influence of land**
 833 **surface parameters cannot be excluded. A corresponding analysis is beyond the scope**
 834 **of this paper, though, and is planned for the future. As a reservation, the expression**
 835 **“self-excited” is used with quotation marks in this text.**

836 Further **oscillation** properties are as follows: Many of the periods appear to be robust,
 837 i.e. they are found with similar values in different models. The periods cover a wide range
 838 from 2 to above 200 years (at least). The different oscillations have similar vertical
 839 profiles (up to 110 km) of amplitudes and phases. This may indicate three-dimensional
 840 atmospheric **oscillation modes excited by some feedback mechanisms**. To clarify this,
 841 latitudinal and longitudinal studies of the oscillations are needed in a future analysis.
 842

843 4.2 The accumulated oscillation amplitudes show a layer structure with alternating maxima
 844 and minima and correlations / anticorrelations in the vertical direction. These appear to be
 845 influenced by the seasonal variations of temperature and zonal wind in the stratosphere,
 846 mesosphere, and lower thermosphere. Table 4 summarizes the results shown in Section 3.5.
 847 Maxima of oscillation amplitudes appear to be associated with westerly (eastward) winds
 848 together with large temperature gradients (positive or negative). Amplitude minima are
 849 associated with either easterly (westward) winds or with near zero temperature gradients. The
 850 latter feature is compatible with a possible vertical displacement mechanism. Such
 851 displacements can be seen, indeed, in the CH₄ data of the HAMMONIA model. The
 852 mechanism summarized in Table 4 appears to be a
 853



854
 855
 856 Fig. 17 Amplitudes of 24 yr and 37 yr oscillations in four subsequent equal time intervals
 857 (Blocks) of the 400 year data set of ECHAM6.
 858

859
 860 basic feature of the atmosphere that influences many different parameters as temperature,
 861 mixing ratios, etc. Vertical displacements of measured temperature profiles have been
 862 discussed for instance by Kalicinsky et al. (2018).
 863

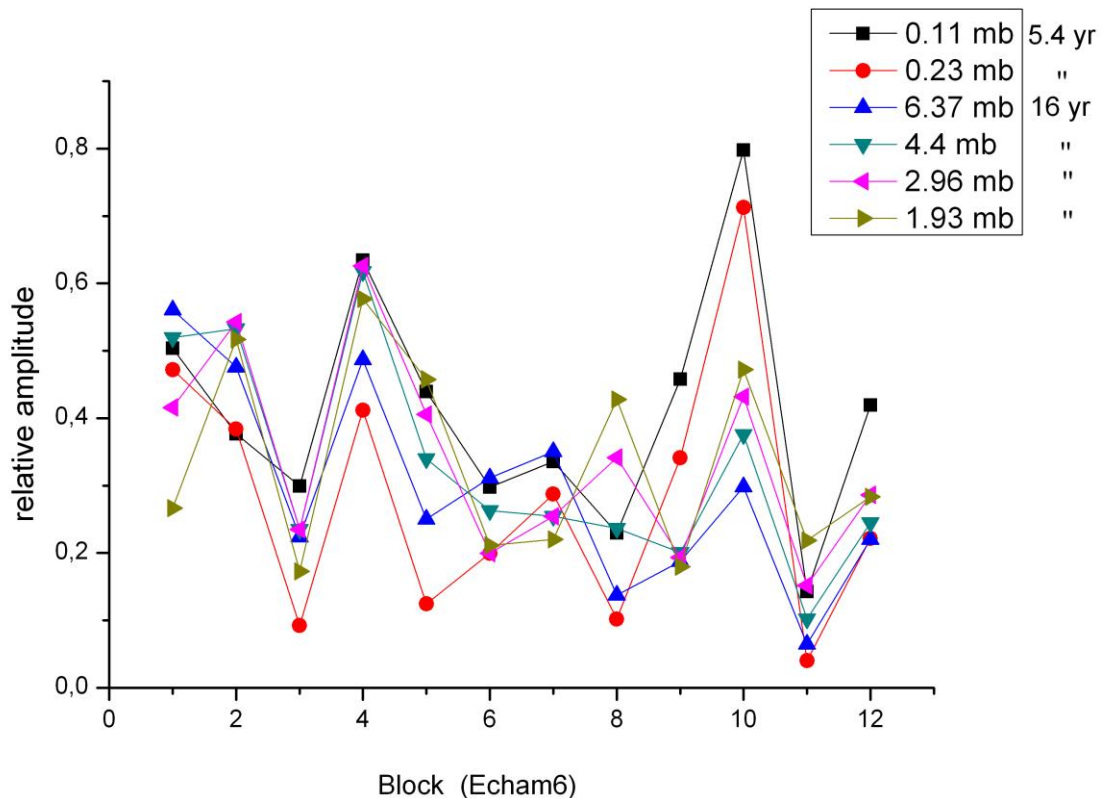
864 4.3 The amplitudes found for the **long-period** oscillations are relatively small (Fig. 1). The
 865 question therefore arises whether these oscillations might be spurious peaks, i.e. some sort of
 866 noise. We tend to deny the question for the following reasons:

867
 868 (a) An accidental agreement of periods as close together as those shown in Table 2a for
 869 different model computations appears very unlikely. This also applies to the Hohenpeißenberg
 870 data in Table 2a, and several of these periods are even found in the GLOTI data.

871 If the period values were accidental they should be evenly distributed over the
 872 period-space. To study this the range of ECHAM6 periods is
 873 considered. Table 2a shows that the error bars (standard deviations) of ECHAM6
 874 cover approximately half of this range. If the periods of this and some other data set occur at
 875 random, half of them should coincide with the ECHAM6 periods within the
 876 ECHAM6 error bars, and half of them should not. This is checked by means of the
 877 WACCM model data, the Hohenpeissenberg measured data, and three further
 878 measurements sets that reach back to 1783 (Innsbruck, 47.3°N;11.4°E; Vienna,
 879 48.3°N;16.4°E; Stockholm, 59.4°N;18.1°E). The result is that about two thirds of the
 880 periods coincide with ECHAM6 periods within the ECHAM6 error bars. This is far
 881 from an even distribution.

882 It is important to note that the data sets used here are quite different in nature: They are
 883 either model simulations with fixed or partially fixed boundaries, or they are real atmospheric
 884 measurements at different locations.

885
 886



887
 888
 889 Fig. 18 FFT amplitudes of 5.4 yr and 16 yr oscillations in 12 equal time intervals (32 yr
 890 blocks) of the ECHAM6 400 year data set.

891
 892

893 A further argument against noise is the distribution of the data in Fig. 9 and 10. If our
894 oscillations were noise, the counts in these Figures should be evenly distributed with respect
895 to the period scale. However, the distribution is highly uneven, with high peaks and large
896 gaps, which is very unlikely to result from noise.
897

898 (b) The periods given in Table 2a were all calculated by means of harmonic analyses
899 (Levenberg-Marquardt algorithm). This was done to support the reliability of the comparison
900 of the three models and four measured data sets. There could be, however, the risk of a
901 “common mode failure”. The harmonic analysis results are therefore checked, and are
902 confirmed by the Lomb-Scargle and autocorrelative spectral (ASA) analyses shown in Fig. 8
903 and 12, and by the above cited results of Plaut et al. (1995) and Meyer and Kantz (2019).
904 There is, however, not a one-to-one correspondence of these numbers and those of Table 2a.
905 In general the number of oscillations found by the harmonic analysis is larger. Hence several
906 of the Table 2a periods might be considered questionable. It is also not certain that Table 2a is
907 exhaustive. Nevertheless, the large number of close coincidences is surprising.
908

909 (c) The layered structure of the occurrence of the oscillations (e.g. Fig. 11a) and the
910 corresponding anti-correlations appear impossible to reconcile with a noise field. These
911 correlations extend over about 20 km (or more) in the vertical which is about three scale
912 heights. Turbulent correlation would, however, be expected over one transport length, i.e. one
913 scale height, only.
914

915 (d) The apparent relation of the oscillations to the zonal wind field and the vertical
916 temperature structure (Table 4) would be very difficult to be explained by noise.
917

918 (e) The close agreement (within single error bars) of the oscillation periods in
919 temperatures and in CH₄ mixing ratios would also be very difficult to be explained by
920 noise.
921

922 In summary it appears that many of the oscillations are intrinsic properties of the
923 atmosphere that are also found in sophisticated simulations of the atmosphere.
924
925

926 4.4 The **long period** oscillations are studied here mainly for atmospheric temperatures.
927 They show up, however, in a similar way in other parameters as winds, pressure, trace gas
928 densities, NAO, etc. (Offermann et al., 2015). Some of the periods in Table 2a appear to be
929 similar to the internal decadal variability of the atmosphere/ocean system (e.g., Meehl et al.,
930 2013; 2016; Fyfe et al. 2016). One example is the Atlantic Multidecadal Oscillation (AMO)
931 as discussed by Deser et al. (2010) with time scales of 65-80 yr, and with its “precise nature
932 ...still being refined”. Variability on centennial time scales and its internal forcing was
933 recently discussed by Dijkstra and von der Heydt (2017). It needs to be emphasized that the
934 oscillations discussed in the present paper are not caused by the ocean as they occur even if
935 the ocean boundaries are kept constant.
936

937 4.5 The **long-period** oscillations obviously are somehow related to the “internal
938 variability” discussed in the atmosphere/ocean literature at 40 – 80 years time scales (“climate
939 noise”, see e.g. Deser et al., 2012, Gray et al., 2004, and other references in Section 1). The
940 particular result of the present analysis is its extent from the ground up to 110 km, showing
941 systematic structures in all of this altitude regime. These vertical structures lead us to hope
942 that the nature of the oscillations and hence of (part of) the “internal variability” can be
943 revealed in the future.

944
945
946
947
948
949
950
951
952
953
954
955
956
957
958
959
960
961
962
963
964
965
966
967
968
969
970
971
972
973
974
975
976
977
978
979
980
981
982
983
984
985
986
987
988
989
990
991
992
993
994

4.6 It appears that the time persistency of the **long period** oscillations is limited. Longer data sets are needed to study this further.

4.7 The internal variability in the atmosphere/ocean system “...makes an appreciable contribution to the total... uncertainty in the future (simulated) climate response...” (Deser et al., 2012). Similarly our **long period** oscillations might interfere with long term (trend) analyses of various atmospheric parameters. This includes slow temperature increases as part of the long term climate change, and needs to be studied further.

5 Summary and Conclusions

The atmospheric structures analyzed in this paper are supposed to be oscillations that are self-generated by some feedback mechanism. The oscillations occur in a similar way in different atmospheric climate models, and even when the boundary conditions of sun, ocean, and greenhouse gases are kept constant. They also occur in long-term temperature measurements series. They are characterized by a large range of period values from below 5 to beyond 200 years. Periods of self-excited oscillations are known to be robust. This is in line with the fact that we find very nearly the same periods in different climate model calculations as well as in long observation series.

As we do not yet understand the nature of the oscillation structures we try to assemble as many of their properties as possible. The oscillations show typical and consistent structures in their vertical profiles. Temperature amplitudes show a layered behaviour in the vertical direction with alternating maxima and minima. Phase profiles are also layered with 180° phase jumps near the altitudes of the amplitude minima (anticorrelations). There are also indications of vertical transports suggesting a displacement mechanism in the atmosphere. As an important result we find that for all oscillation periods the altitude profiles of amplitudes and phases as well as the displacement heights are nearly the same. This leads us to suspect an atmospheric oscillation mode.

These signatures are found to be related to the thermal and dynamical structure of the middle atmosphere. They are seen to be an essential part of atmospheric dynamics. **Land surface influences in addition need to be studied in the future.** All results presently available are local, i.e. they refer to the latitude and longitude of Central Europe. In a future step horizontal investigations need to be performed to check on a possible modal structure.

Most of the present results are for temperatures at various altitudes (up to 110 km). Other atmospheric parameters indicate a similar behaviour and need to be analyzed in detail in the future. Also, the potential of the long period oscillations to interfere with trend analyses needs to be investigated.

995
996
997
998
999
1000
1001
1002
1003
1004
1005
1006
1007
1008
1009
1010
1011
1012
1013
1014
1015
1016
1017
1018
1019
1020
1021
1022
1023
1024
1025
1026
1027
1028
1029
1030
1031
1032
1033
1034
1035
1036
1037
1038
1039
1040
1041
1042
1043
1044
1045

Author contribution

DO performed data analysis and prepared the manuscript and figures with contributions from all co-authors.

JW managed data collection and performed FFT spectral analyses.

ChK performed Lomb-Scargle spectral and statistical analyses

RK provided interpretation and editing of the manuscript, figures, and references.

Competing Interests

The authors declare that they have no conflict of interest.

1046
1047
1048
1049
1050
1051
1052
1053
1054
1055
1056
1057
1058
1059
1060
1061
1062
1063
1064
1065
1066
1067
1068
1069
1070
1071
1072
1073
1074
1075
1076
1077
1078
1079
1080
1081

Acknowledgements

Global Land Ocean Temperature Index (GLOTI) data were downloaded from http://data.giss.nasa.gov/gistemp/tabledata_v3/GLB.Ts+dSST.txt and are gratefully acknowledged..

We thank Katja Matthes (GEOMAR, Kiel, Germany) for making available the WACCM4 data, and for helpful discussions. Model integrations of the CESM-WACCM Model have been performed at the Deutsches Klimarechenzentrum (DKRZ) Hamburg, Germany. The help of Sebastian Wahl in preparing the CESM-WACCM data is greatly appreciated.

HAMMONIA and ECHAM6 simulations were performed at and supported by the German Climate Computing Centre (DKRZ). Many and helpful discussions with Hauke Schmidt (MPI Meteorology, Hamburg, Germany) are gratefully acknowledged.

We are grateful to Wolfgang Steinbrecht (DWD, Hohenpeißenberg Observatory, Germany) for the Hohenpeißenberg data and many helpful discussions.

Part of this work was funded within the project MALODY of the ROMIC program of the German Ministry of Education and Research under Grant No. 01LG1207A

We thank three referees for their detailed and thoughtful comments.

1082
1083
1084
1085
1086
1087
1088
1089
1090
1091
1092
1093
1094
1095
1096
1097
1098
1099
1100
1101
1102
1103
1104
1105
1106
1107
1108
1109
1110
1111
1112
1113
1114
1115
1116
1117
1118
1119
1120
1121
1122
1123
1124
1125
1126
1127
1128
1129
1130
1131

References.

- Biondi, F., Gershunov, A., and Cayan, D.R.: North Pacific Decadal Climate Variability since 1661, *J. Climate* 14, 5-10, 2001.
- Dai, A, Fyfe, J.C., Xie, Sh.-P., and Dai, X,: 2015.: Decadal modulation of global surface temperature by internal climate variability, *Nature Climate Change*, doi:10.1036/NCLIMATE2605 , 2015.
- Deser, C. Alexander, M.A., Xie,S.P., Phillips, A.S.: Sea surface temperature variability: patterns and mechanisms, *Ann. Rev. Mar. Sci.*,2, 115-143, 2010.
- Deser, C., Phillips, A., Bourdette, V., and Teng, H.: Uncertainty in climate change projections: the role of internal variability, *Clim. Dyn.*, 38, 527-546, 2012.
- Deser, C., Phillips, A.S., Alexander, M.A., and Smoliak, B.V.: Projecting North American climate over the next 50 years: Uncertainty due to internal variability, *J.Climate*, 27, 2271-2296, 2014.
- Dijkstra, H.A., te Raa, L., Schmeits, M., and Gerrits, J.: On the physics of the Atlantic Multidecadal Oscillation, *Ocean Dynamics*, DOI: 10/1007/s10236-005-0043-0, 2005.
- Dijkstra, H.A., and von der Heydt, A.S.: Basic mechanisms of centennial climate variability, *Pages Magazine*, Vol.25, No.3, 2017.
- Flato, G., et al. : Evaluation of Climate Models, in: *Climate Change 2013: The Physical Science Basis, Contribution of Working Group I to the Fifth Assessment Report of the Intergovernmental Panel on Climate Change*, (eds..Stocker, T.E., et al.) Ch.9, IPCC, Cambridge Univ.Press, UK and New York, NY, USA, 2013.
- Fyfe, J. C., Meehl, G.A., England, M.H., Mann, M.E., Santer, B.D., Flato, G.M., Hawkins, E., Gillett, N.P., Xie, Sh.P., Kosaka, Y., and Swart, N.C.: Making sense of the early-2000s warming slowdown, *Nature Climate Change*, 6, 224-228, 2016.
- Giorgetta, M. et al.: Climate and carbon cycle changes from 1850 to 2100 in MPI-ESM simulations for the coupled model intercomparison project phase 5, *J. Adv. Model. Earth Syst*, 5, 572-597, doi:10.1002/jame.20038, 2013.
- Gray, ST.T., Graumlich, L.J., Betancourt, J.L., and Pederson, G.T.: A tree-ring based reconstruction of the Atlantic Multidecadal Oscillation since 1567 A.D.. *Geophys.Res.Lett.*, 31, L 2205, doi:10.1029/2004GL019932 2004.

1132 Hansen, F., Matthes, K., Petrick, C., and Wang, W.: 2014. The influence of natural and
1133 anthropogenic factors on major stratospheric sudden warmings. *J.Geophys.Res. Atmos.*, 119,
1134 8117-8136, 2014.

1135
1136 Hansen, J., Ruedy, Sato, M., and Lo, K.: Global Surface Temperature Change, *Rev.Geophys.*,
1137 48, RG 4004, 2010.

1138
1139 Kalicinsky, Ch., Knieling, P., Koppmann, R., Offermann, D., Steinbrecht, W., and Wintel,
1140 J.: 2016. Long term dynamics of OH* temperatures over Middle Europe: Trends and solar
1141 correlations, *Atmos. Chem. Phys.*, 16, 15033 – 15047, 2016.

1142
1143 Kalicinsky, CH., Peters, D.H.W., Entzian, G., Knieling, P., and Matthias, V.: Observational
1144 evidence for a quasi-bidecadal oscillation in the summer mesopause region over Western
1145 Europe, *J. Atmos. Sol.-Terr. Phys*, 178, 7 – 16., doi.org/10.1016/j.jastp.2018.05.008, 2018.

1146
1147 Karnauskas, K. B., Smerdon, J.E., Seager, R., and Gonzalez-Rouco, J.F. : A pacific centennial
1148 oscillation predicted by coupled GCMs, *JCLI* September 2012, doi:10.1175/JCLI-D-11-
1149 00421.1, 2012.

1150
1151 Kinnison, D., Brasseur, G.P., Walters, S., et al. : Sensitivity of chemical tracers to
1152 meteorological parameters in the MOZART-3 chemical transport model. *J.Geophys.Res.*,
1153 112, D20302, doi :10.1029/2006JD007879, 2007.

1154
1155 Latif, M., Martin, T., and Park, W.: Southern ocean sector centennial climate variability and
1156 recent decadal trends, *J. Climate*, 26, 7767-7782, 2013.

1157
1158 Lean,J., Rottman, G., Harder, J., and G.Knopp, G.: SOURCE contributions to new
1159 understanding of global change and solar variability, *Sol.Phys.* 230, 27-53.
1160 doi:10.1007/S11207-005-1527-2, 2005.

1161
1162 Lomb, N.R., Least-squares frequency analysis of unequally spaced data, *Astrophys.Space*
1163 *Sci.*, 39, 447-462, 1976.

1164
1165 Lu, J., Hu, A., and Zeng, Z.: On the possible interaction between internal climate variability
1166 and forced climate change, *Geophys. Res. Lett.*, 41, 2962-2970, 2014.

1167
1168 Mantua, N.J., and Hare, St.R.: ThePacific Decadal Oscillation. *J.Oceanography*, 58, 35,2002.

1169
1170 Matthes, K., Kodera, K., Garcia, R.R., Kuroda, Y., Marsh, D.R., and Labitzke, K.: The
1171 importance of time-varying forcing for QBO modulation of the atmospheric 11 year solar
1172 cycle signal, *J.Geophys.Res.*, 118, 4435-4447, 2013.

1173
1174 Meehl, G.A., Hu, A., Arblaster, J., Fasullo, J., and Trenberth, K.E.: Externally forced and
1175 internally generated decadal climate variability associated with the Interdecadal Pacific
1176 Oscillation, *J.Cimate*, 26, 7298-7310, 2013.

1177
1178 Meehl, G.A., Hu, A., Santer, B.D., and Xie, SH.-P.: Contribution of Interdecadal Pacific
1179 Oscillation to twentieth-century global surface temperature trends. *Nature Climate Change*,
1180 6,1005-1008, doi:10.1038/nclimate3107, 2016.

1181

1182 Meyer, P.G., and Kantz, H.: A simple decomposition of European temperature variability
1183 capturing the variance from days to a decade, *Climate Dynamics*, 53, 6909-6917,
1184 doi.org/10.1007/s00382-019-04965-0, 2019.

1185
1186 Minobe, Sh.: A 50-70 year climatic oscillation over the North Pacific and North America,
1187 *Geophys.Res.Lett.*, 24, 683-686, 1997.

1188
1189 Offermann, D., Goussev, O., Kalicinsky, Ch., Koppmann, R., Matthes, K., Schmidt, H.,
1190 Steinbrecht, W., and J. Wintel, J.: A case study of multi-annual temperature oscillations in
1191 the atmosphere: Middle Europe, *J.Atmos.Sol.-Terr.Phys.*, 135, 1-11, 2015.

1192
1193 Plaut, G., Ghil, M., and Vautard, R.: Interannual and interdecadal variability in 335 years of
1194 Central England Temperatures, *Science*, 268, 710 – 713, 1995.

1195
1196 Paul, A., and M. Schulz, M.: Holocene climate variability on centennial-to-millennial time
1197 scales: 2. Internal and forced oscillations as possible causes. In: Wefer,G., W.Berger, K-E.
1198 Behre, and E. Jansen (eds), 2002, *Climate development and history of the North Atlantic*
1199 *realm*, Springer, Berlin, Heidelberg, 55-73, 2002.

1200
1201 Polyakov,I.V. Berkryaev, R.V., Alekseev,G.V., Bhatt, U.S., Colony, R.L., Johnson, M.A.,
1202 Maskstas, A.P., and Walsh, D.: Variability and trends of air temperature and pressure in the
1203 Maritime Arctic, 1875-2000, *J.Climate*, 16, 2067-2077, 2003.

1204
1205 Roeckner, E., Brokopf, R., Esch, M., Giorgetta, M., Hagemann, S., Kornblueh, L., Manzini,
1206 E., Schlese, U., Schulzweida, U.: Sensitivity of simulated climate to horizontal and vertical
1207 resolution in the ECHAM5 atmosphere model, *J.Clim.*, 19, 3771–3791, 2006.

1208
1209 Scargle, J.D.: Studies in astronomical time series analysis. II. Statistical aspects of spectral
1210 analysis of unevenly spaced data, *Astrophys.J.*, 263, 835-853, 1982.

1211
1212 Schlesinger, M.E. and N. Ramankutty, N.: An oscillation in the global climate system of
1213 period 65-70 years, *Nature*, 367, 723-726, 1994.

1214
1215 Schmidt, H., Brasseur, G.P., Charron, M., Manzini, E., Giorgetta, M.A., Diehl,T., Fo-
1216 michev, V.I., Kinnison, D., Marsh, D., Walters, S.: The HAMMONIA chemistry climate
1217 model: Sensitivity of the mesopause region to the 11-year solar cycle and CO2 doubling, *J.*
1218 *Clim*, 19, 3903–3931, <http://dx.doi.org/10.1175/JCLI3829.1>, 2006.

1219
1220 Schmidt, H., Brasseur, G.P., and Giorgetta, M.A.:2010. The solar cycle signal in a general
1221 circulation and chemistry model with internally generated quasi-biennial oscillation. *J.*
1222 *Geophys. Res.* 115, 8, doi :10.1029/2009JD012542, 2010.

1223
1224 Schönwiese, Ch.-D.: *Praktische Statistik für Meteorologen und Geowissenschaftler*,
1225 2.Auflage, Gebrüder Borntraeger, Berlin, Stuttgart, Abb.57, page 185, [www.borntraeger-](http://www.borntraeger-cramer.de/9783443010294)
1226 [cramer.de/9783443010294](http://www.borntraeger-cramer.de/9783443010294), 1992.

1227
1228 Soon, W. W.-H.: Variable solar irradiance as a plausible agent for multidecadal variations in
1229 the Arctic-wide surface air temperature record of the past 130 years, *Geophys.Res.Lett.*, 32,
1230 L16712, doi:10.1029/2005GL023429 2005.

1231

1232 Stevens, B., Giorgetta, M., Esch, M., Mauritsen, T., Crueger, T., Rast, S., Salzmann, M.,
1233 Schmidt, H., Bader, J., Block, K., Brokopf, R., Fast, I., Kinne, S., Kornblueh, L., Lohmann,
1234 U., Pincus, R., Reichler, T., and Roeckner, E.: The atmospheric component of the MPI-M
1235 earth system model: ECHAM6, *J. Adv. Model. Earth Syst.*, 5, 1-27, 2013.
1236
1237 White, W.B., and Liu, Z.: Non-linear alignment of El Nino to the 11-yr solar cycle,
1238 *Geophys.Res.Lett.*, 35, L19607, doi:10.1029/2008GL034831, 2008.
1239
1240 Xu, D., Lu, H., Chu, G., Wu, N., Shen, C., Wang, C., and Mao, L.: 500-year climate cycles
1241 stacking of recent centennial warming documented in an East Asian pollen record,
1242 *Scientific Reports* , 4, No.3611, doi:10.1038/srep03611, 2014.
1243
1244
1245
1246
1247
1248
1249
1250
1251
1252
1253
1254
1255
1256
1257
1258
1259
1260
1261
1262
1263
1264
1265
1266
1267
1268
1269
1270
1271
1272
1273
1274
1275
1276
1277
1278
1279
1280
1281
1282
1283

1284
 1285
 1286
 1287
 1288
 1289
 1290
 1291
 1292
 1293
 1294
 1295
 1296
 1297
 1298
 1299
 1300
 1301
 1302
 1303
 1304
 1305
 1306
 1307
 1308
 1309
 1310
 1311
 1312
 1313
 1314
 1315
 1316
 1317
 1318
 1319
 1320
 1321
 1322
 1323
 1324
 1325
 1326
 1327
 1328
 1329
 1330
 1331
 1332
 1333
 1334
 1335
 1336
 1337
 1338
 1339
 1340

Table 1

Properties of the GCM simulations

All data are for Central Europe (50°N, 7°E). For various details see text.

	HAMMONIA	WACCM4	ECHAM6
Horizontal resolution	T31	1.9°x2.5° (lat/long)	T63
Vertical resolution	119 levels 1 km (stratosphere)	66 levels	47 levels
altitude range	0 – 110 km	0 – 108 km	0 – 78 km
length of simulation	34 yr	150 yr	400 yr
time resolution of data used	annual/monthly	annual	annual
boundary conditions			
- sun	fixed	variable (see text)	fixed
- ocean	climatological SST and sea ice	climatological SST and sea ice	climatological SST and sea ice
- greenhouse gases	fixed	fixed (1960 values)	fixed
References	Schmidt et al., 2010	Hansen et al., 2014	Stevens et al., 2013

1341
 1342
 1343
 1344
 1345
 1346
 1347
 1348
 1349
 1350
 1351
 1352
 1353
 1354
 1355
 1356
 1357
 1358
 1359
 1360
 1361
 1362
 1363
 1364
 1365
 1366
 1367
 1368
 1369
 1370
 1371
 1372
 1373
 1374
 1375
 1376
 1377
 1378
 1379
 1380
 1381
 1382
 1383
 1384
 1385
 1386
 1387
 1388
 1389
 1390
 1391
 1392
 1393

Table 2a:

Periods of temperature oscillations from harmonic analyses

Periods are numbered according to increasing values. Periods (in years) are given with their standard deviations. "Self-excited" periods are from the HAMMONIA, WACCM, and ECHAM6 models, respectively. Additional periods are from Hohenpeißenberg measurements, and from the Global Land Ocean Temperature Index (GLOTI).

HAMMONIA periods are limited to 28.5 yr as the model run covered 34 yr, only.

WACCM periods are given below 147 yr from a model run of 150 yr. ECHAM6 periods are from a 400 yr run.

Short periods (below 20 yr) are not shown for WACCM, ECHAM6, and GLOTI as they are not used in the present paper. Hohenpeißenberg and GLOTI data after 1980 are not included in the analyses because of their steep increase in later years.

Periods given in bold type refer to Tab. 2b.

No	HAMMONIA (119 layers) (years)		WACCM (years)		ECHAM6 (47 layers) (years)		Hohenpeißenberg 1783 – 1980 (years)		GLOTI 1880 - 1980 (years)	
1	5.34	± 0.1					5.48	±0.21		
2	6.56	0.24					6.16	0.20		
3	7.76	0.29					7.83	0.26		
4	9.21	0.53					9.50	0.65		
5	10.8	0.34					10.85	0.38		
6	13.4	0.68					13.6	0.80		
7	17.3	1.05					18.02	1.08		
8	--	--			20.0	±0.35	19.9	± 1	20.2	± 1.36
9	--	--			20.9	0.15	--	--		
10	22.8	1.27	21.7	± 1.02	22.1	0.23	21.9	0.94		
11	--	--			23.8	0.42				
12	--	--	25.82	0.86	25.3	0.46	25.1	0.62	25.5	2.0
13	28.5	1.63	--	--	27.3	0.41	--	--		
14			31.56	1.42	30.2	0.49	29.8	0.66		
15			--	--	33.3	0.84	--	--		
16			38.1	0.82	36.9	1.17	36.01	1.28	35.4	2.42
17			41.89	0.95	41.4	0.97	--	--		
18			--	--	48.4	1.73	--	--		
19			--	--	--	--	52.06	1.61	53.4	11.4
20			57.64	1.69	58.3	1.77	--	--		
21			66.95	7.31	64.9	2.98	--	--		
22			--	--	77.5	3.94	81.6	4.18		
23			97.27	5.06	95.5	5.86	--	--		
24			147	14.9	129.4	14.5	--	--		
25					206.7	16.3	--	--		
26					--	--	238.2	11.8		

1394
1395
1396
1397
1398
1399
1400
1401
1402
1403
1404
1405
1406
1407
1408
1409
1410
1411
1412
1413
1414
1415
1416
1417
1418
1419
1420
1421
1422
1423
1424
1425
1426
1427
1428
1429
1430
1431
1432
1433
1434
1435
1436
1437
1438
1439
1440
1441
1442
1443
1444
1445
1446
1447
1448
1449
1450
1451
1452
1453
1454

Table 2b Comparative periods (in years)

Period (yr) from HAMMONIA/ECHAM6 (numbers refer to Tab. 2a)	Accuracy/Significance (SSA: Single Spectrum Analysis) (ASA: Auto correlation Spectral Analysis) (DFA: Detrended Fluctuation Analysis)	Source/corresponding period
#1 5.34 ± 0.1	2 σ	- Lomb-Scargle periodogram as in Fig. 8 (not shown here)
	SSA	- Plaut et al. (1995) : 5.2 yr
#2 6.56 ± 0.24	1 σ	- Lomb-Scargle periodogram as in Fig.8 (not shown here)
		- see also CH4 analysis (Tab.3): 6.43 + 0.26 yr
#3 7.76 ± 0.29	SSA	- Plaut et al. (1995) : 7.7 yr
	ASA (80 %)	- Schönwiese (1992) : 7.5 yr
	DFA	- Meyer and Kantz (2019) : 7.6 ±1.8 yr
#6 13.4 ± 0.68	SSA	- Plaut et al. (1995) : 14.2 yr
	ASA (95%)	- Schönwiese (1992): 13 yr
	2 σ	- Lomb-Scargle periodogram as in Fig.8 (not shown here)
		- see also CH4 analysis (Tab.3) : 13.73 ± 0.93 yr
#7 17.3 ± 1.05	2 σ	- Lomb-Scargle periodogram as in Fig. 8 (not shown here)
#10 21.1 ± 0.23	1 σ	- Lomb-Scargle periodogram : 22.3 yr , see Fig.8
#12 25.3 ± 0.46	SSA	- Plaut et al. (1995) : 25.0 yr
#14 30.2 ± 0.49	2 σ	- Lomb-Scargle periodogram : 30.4 yr see Fig.8
#17 41.4 ± 0.97	2 σ	- Lomb-Scargle periodogram : 40.7 yr see Fig.8
#18 48.4 ± 1.73	2 σ	- Lomb-Scargle periodogram : 48.1 yr see Fig.8
#20 58.3 ± 1.77	1 σ	- Lomb-Scargle periodogram: 58.9 yr see Fig. 8

1455
 1456
 1457
 1458
 1459
 1460
 1461
 1462
 1463
 1464
 1465
 1466
 1467
 1468
 1469
 1470
 1471
 1472
 1473
 1474
 1475
 1476
 1477
 1478
 1479
 1480
 1481
 1482
 1483
 1484
 1485
 1486
 1487
 1488
 1489
 1490
 1491
 1492
 1493
 1494
 1495
 1496
 1497
 1498
 1499
 1500
 1501
 1502
 1503
 1504
 1505
 1506

Table 3

Period comparison of two different HAMMONIA runs: temperature and CH4

Periods (in years) are given together with their standard deviations.

HAMMONIA run Hhi-max (temperature and CH4 mixing ratios) uses 119 altitude layers and covers 34 years; run Hlo-max uses 67 layers and covers 20 years.

No	Hhi-max (temperature)		Hlo-max (temperature)		CH4	
1	2.06	± 0.02	2.07	± 0.04		
2	2.16	0.02	2.15	0.02		
3	2.33	0.04	2.36	0.03		
4	2.51	0.04	2.43	0.02		
5	2.79	0.08	2.78	0.07		
6	3.11	0.08	3.2	0.09		
7	3.52	0.12	3.44	0.15	3.56	± 0.15
8	3.96	0.08	3.9	0.12	4.02	0.17
9	4.48	0.21	4.27	0.21	4.57	0.17
10	5.34	0.1	5.48	0.29	5.41	0.29
11	6.56	0.24	6.57	0.29	6.43	0.26
12	7.76	0.29	8.02	0.12	7.9	0.45
13	9.21	0.53	9.16	0.33	9.38	0.47
14	10.8	0.34	11.05	0.46	10.93	0.61
15	13.4	0.68	13.02	0.83	13.73	0.93
16	17.3	1.05	--	--	16.75	0.9
17	22.8	1.27	22.68	1.11		

1507
1508
1509
1510
1511
1512
1513
1514
1515
1516
1517
1518
1519
1520
1521
1522
1523
1524
1525
1526
1527
1528
1529
1530
1531
1532
1533
1534
1535
1536
1537
1538
1539
1540
1541
1542
1543
1544
1545
1546
1547
1548
1549
1550
1551
1552
1553
1554
1555
1556
1557

Table 4

Maxima / minima of accumulated amplitudes of temperature oscillations and associated structures (see Fig. 11a)
(stratosphere, mesosphere, lower thermosphere)

altitude (km)	accumulated amplitudes	zonal wind	temperature gradient
105	max	westerly (summer)	large (positive)
93	min	westerly (summer)	near zero
84	max	westerly (summer)	large (positive)
78	min	easterly (except Sept)	medium (negative)
63	max	westerly (winter)	large (negative)
51	min	westerly (winter)	near zero
42	max	westerly (winter)	large (positive)

1558
1559
1560
1561
1562
1563
1564
1565
1566
1567
1568
1569
1570
1571
1572
1573
1574
1575
1576
1577
1578
1579
1580
1581
1582
1583
1584
1585
1586
1587
1588
1589
1590
1591
1592
1593
1594
1595
1596
1597
1598
1599
1600
1601
1602
1603
1604
1605
1606
1607
1608
1609
1610
1611
1612
1613
1614

Table 5

List of Acronyms

Acronym

Definition

CCM	Chemistry Climate Model
CESM-WACCM	Community Earth System Model – Whole Atmosphere Community Climate Model
ECHAM6	ECMWF/Hamburg
GLOTI	Global Land Ocean Temperature Index
HAMMONIA	HAMBURG Model of the Neutral and Ionized Atmosphere
IPCC	Intergovernmental Panel on Climate Change
LOTI	Land Ocean Temperature Index